

1 **Short title:** E2FB-RBR function in leaf development

2 **E2FB interacts with RETINOBLASTOMA RELATED and regulates cell proliferation**
3 **during leaf development**

4 Erika Ószi^{a,b*}, Csaba Papdi^{c*}, Binish Mohammed^c, Aladár Petkó-Szandtner^{a,d}, Tünde
5 Leviczky^{a,b}, Eszter Molnár^a, Carlos Galvan-Ampudia^c, Safina Khan^c, Enrique Lopez Juez^c,
6 Beatrix Horváth^{cΔ}, László Bögre^{cΔ}, and Zoltán Magyar^{aΔ+}

7

8 ^a Institute of Plant Biology, Biological Research Centre, Szeged, Hungary

9 ^b Doctoral School in Biology, Faculty of Science and Informatics, University of Szeged,
10 Szeged, Hungary

11 ^c Royal Holloway University of London, School of Biological Sciences, Centre for Systems
12 and Synthetic Biology, Egham, UK.

13 ^d Institute of Biochemistry, Biological Research Centre, Szeged, Hungary

14 ^e Laboratoire de Reproduction et Développement des Plantes, Université de Lyon, CNRS,
15 INRA, F-69364 Lyon, France.

16 * These authors contributed equally.

17 ^Δ Senior authors

18 ⁺ Author for contact: Magyar.Zoltan@brc.hu or magyarz@brc.hu

19 The author responsible for distribution of materials integral to the findings presented in this
20 article in accordance with the policy described in the Instructions for Authors
21 (www.plantphysiol.org) is: Zoltán Magyar (Magyar.Zoltan@brc.hu).

22 ¹ E.Ó., A.P-Sz, T.L., E.M. and Z.M. were supported by the Hungarian Scientific Research
23 Fund (OTKA K-105816) and by the Ministry for National Economy (Hungary, GINOP-
24 2.3.2-15-2016-00001). T.L. was funded by the Young Scientist Fellowship of the Hungarian
25 Academy of Sciences, A.P-Sz. was supported by the GINOP-2.3.2-15-2016-00032. Cs.P and
26 B.M.H. were funded by the Marie Curie IEF fellowships (FP7-PEOPLE-2012-IEF.330713
27 and FP7-PEOPLE-2012-IEF.330789, respectively). Cs.P. and L.B were funded by the
28 BBSRC-NSF grant (BB/M025047/1). The funders had no role in the design of the study, data
29 collection and analysis, decision to publish, or preparation of the manuscript.

30

31 **One-sentence summary:** The main function of the E2FB transcription factor is to restrict
32 cell proliferation and establish quiescence during Arabidopsis leaf development; it acts in a
33 complex with RETINOBLASTOMA-RELATED.

34

35 **Author contributions**

36 The authors have made the following declarations about their contributions:

37

38 Z.M, E.L.J, and L.B conceived the idea and designed the study to analyse the function of
39 E2FB during leaf development. Z.M generated and Z.M and E.Ó. performed the phenotypic
40 analysis and microscopic characterisation of transgenic Arabidopsis lines and mutants; with
41 the exception of the construction of GFP-E2FA^{ARBR}, and GFP-E2FB^{ARBR} and transgenic lines
42 were generated by E.M, and the construction of the 3xvYFP-tagged E2FA and E2FB
43 translational fusions and the generation of these transgenic Arabidopsis lines; these were
44 carried out by S.K. and C.G-A. Immunoblottings, immunoprecipitations (IP) and co-IP were
45 carried out by Z.M., E.Ó., and T.L. ChIP with GFP on *CycD3;1*, *CDKB1;1* and *RBR*
46 promoters was performed by Cs.P. The transcriptional level of the cell cycle genes in the
47 transgenic lines, the ploidy measurement by FCM and the measurement of cell size in
48 cotyledonous leaves was performed by B.M. Cell number, cell size and cellular parameters of
49 the various transgenic lines were determined by E.Ó and E.M. The manuscript was written by
50 B.M.H., L.B., E.L.J and Z.M; seen and commented by all authors.

51

52 **Abstract**

53 Cell cycle entry and quiescence are regulated by the E2F transcription factors in association with
54 RETINOBLASTOMA-RELATED (RBR). E2FB is considered to be a transcriptional activator of cell
55 cycle genes, but its function during development remains poorly understood. Here, by studying E2FB-
56 RBR interaction, E2F target gene expression, and epidermal cell number and shape in *e2fb* mutant and
57 overexpression lines during leaf development in *Arabidopsis thaliana*, we show that E2FB in
58 association with RBR plays a role in the inhibition of cell proliferation to establish quiescence. In
59 young leaves, both RBR and E2FB are abundant and form a repressor complex that is reinforced by
60 an autoregulatory loop. Increased E2FB levels either by expression driven by its own promoter or
61 ectopically together with DIMERISATION PARTNER A, further elevates the amount of this
62 repressor complex, leading to reduced leaf cell number. Cell overproliferation in *e2fb* mutants and in
63 plants overexpressing a truncated form of E2FB lacking the RBR binding domain strongly suggested
64 that RBR repression specifically acts through E2FB. The increased number of small cells below the
65 guard cells and of fully developed stomata indicated that meristemoids preferentially hyperproliferate.
66 As leaf development progresses and cells differentiate, the amount of RBR and E2FB gradually
67 declined. At this stage, elevation of E2FB level can overcome RBR repression leading to the
68 reactivation of cell division in pavement cells. In summary, E2FB in association with RBR is central
69 to regulating cell proliferation during organ development to determine final leaf cell number.

70

71 **Introduction**

72 The time window for cell proliferation is the most fundamental determinant for meristem size
73 and has the largest impact on final organ size (Gazquez and Beemster, 2017). This is set by
74 the coordination of cell cycle and exit to differentiation that are governed through complex
75 regulatory mechanisms culminating on the evolutionarily conserved Retinoblastoma (Rb)
76 repressor protein and the E2F transcription factor targets (van den Heuvel and Dyson, 2008).
77 According to the textbook model established in animal systems, cell cycle entry is guarded by
78 cyclin dependent kinases (CDKs), which, upon activation by mitogenic signals,
79 phosphorylate and thereby inactivate Rb and other related pocket proteins. When released
80 from Rb repression, the so-called activator E2Fs drive the cell cycle by activating the
81 expression of cell cycle genes required for the G1 to S-phase transition. By contrast, the
82 repressor-type E2Fs function together with Rb to instigate quiescence and to allow
83 differentiation (Morgan, 2007).

84 In *Arabidopsis thaliana* (Arabidopsis), a single gene codes for the RETINOBLATOMA
85 RELATED (RBR), and this protein acts through three E2F transcription factors, known as
86 E2FA, E2FB, and E2FC. These three E2Fs can only bind to DNA in complex with the
87 DIMERISATION PARTNER A or B (DPA or DPB, De Veylder et al., 2007). Modelling
88 Arabidopsis E2Fs on the animal scenario places E2FA and E2FB as activators and E2FC as a
89 repressor, but similar to animal cells, this subdivision is largely supported by overexpression
90 studies (Magyar et al., 2016). Ectopic co-overexpression of E2FB with DPA allows the
91 continued proliferation of cultured tobacco (*Nicotiana tabacum*) cells in the absence of the
92 plant growth hormone auxin (Magyar et al., 2005). This is reminiscent of the effect of human
93 E2F1 overexpression, which triggers S-phase entry in growth factor-deprived cultured cells
94 (Johnson et al., 1993). Overexpression of E2FB without the DP partner also leads to the
95 upregulation of cell cycle genes and surprisingly a much reduced root growth both in
96 Arabidopsis (Sozzani et al., 2006) and in tomato (*Solanum lycopersicum*; Abraham and del
97 Pozo, 2012), with fruit size increased in the latter. E2FB is expressed throughout the cell
98 cycle phases (Magyar et al., 2000; Mariconti et al., 2002; Magyar et al., 2005) and has the
99 ability to drive both the G1 to S and G2 to M transitions, leading to shortened cell doubling
100 time and reduced cell sizes (Magyar et al., 2005). The accelerated entry into mitosis was
101 correlated with the induced expression of the G2-M specific CDKB1;1, following E2FB
102 overexpression (Magyar et al., 2005; Henriques et al., 2013). The activity of E2FB is tightly

103 controlled by RBR phosphorylation in response to sucrose availability, overexpression of
104 CYCLIN D3;1 (CYCD3;1), or the counteracting CDK inhibitor KIP-RELATED PROTEIN 2
105 (KRP2; Magyar et al., 2012).

106 E2FA differs from E2FB in many respects: (1) E2FA is most abundant in S-phase cells, (2)
107 when overexpressed, it can promote cell proliferation in meristematic cells, whereas in cells
108 that have lost cell division competence, E2FA overexpression supports a modified cell cycle
109 with repeated S-phases, called endoreduplication, and (3) the association of E2FA with RBR
110 is not disrupted, but rather enhanced when cell proliferation is induced by excess sucrose or
111 overexpression of CYCD3;1 (De Veylder et al., 2002; Magyar et al., 2012). Furthermore,
112 E2FA function in endoreduplication does not rely on promoting the transcription of S-phase
113 genes through the trans-activation domain, but rather on the ability of E2FA to associate with
114 RBR and to repress genes regulating the entry into endoreduplication and cell differentiation
115 (Magyar et al., 2012). Therefore, it was suggested that E2FA in association with RBR plays a
116 role in maintaining cell proliferation competence in meristems. In addition, E2FA was shown
117 to play roles in maintaining genome integrity and viability in meristematic cells (Horvath et
118 al., 2017).

119 E2FA and E2FB appear to be redundantly required for cell proliferation because no viable
120 plants can be generated when predictably null mutants are combined (Li et al., 2017).
121 However, a viable double *e2fab* mutant plant was generated by combining different loss-of-
122 function mutant alleles for E2FA (*e2fa-2*) and E2FB (*e2fb-1*; Heyman et al., 2011),
123 suggesting that at least the C-terminal transactivation function of these E2Fs are dispensable
124 for plant growth and development.

125 The repressor function of E2FC is supported by its overexpression that suppressed
126 meristematic cell divisions and the expression of mitotic CYCB1;1, and by its silencing that
127 led to the upregulation of both the S-phase associated *HISTONE 4 (H4)* and *CELL DIVISION*
128 *CYCLE 6 (CDC6)* and the mitotic *CYCB1;1* genes (del Pozo et al., 2006). In mammalian
129 cells, the DP, RB-like, E2F4, and Multi-vulval class B (MuvB) multiprotein complex, known
130 as DREAM, acts as a repressor on cell cycle genes to impose quiescence (Sadasivam and
131 DeCaprio, 2013). In Arabidopsis, E2FC, RBR, and MYB3R3 (a repressor type MYB3R or
132 Rep-MYB3R) are part of the DREAM complex with a repressive function that establishes
133 quiescence (Kobayashi et al., 2015). However, unique to plants is that the activator type
134 E2FB partners the mitosis specific activator MYB3R4 (an Act-MYB3R) in another DREAM

135 complex (Kobayashi et al., 2015; Harashima and Sugimoto, 2016). This provides additional
136 support for the mitotic role of E2FB.

137 The leaf is an excellent model to study how the coordinated action between cell proliferation
138 and differentiation is regulated (Andriankaja et al., 2012; Kalve et al., 2014). The leaf has a
139 determinate size, and its growth is the result of two partially overlapping processes: the initial
140 cell proliferation followed by cell expansion, which occurs as cells permanently exit the cell
141 cycle. Cell division is differently regulated in distinct cell populations within the leaf
142 epidermis. The meristematic protodermal cells go through formative cell divisions with a cell
143 proliferation front progressively restricted to the base of the leaf during development. When
144 epidermal leaf cells exit mitosis, they become lobed and enlarged in size, which is coupled
145 with an increase in ploidy through a switch from the mitotic cell cycle to the
146 endoreduplication program (De Veylder et al., 2011). A substantial bulk of pavement cells
147 originate from stomata meristemoids interspersed along the leaf surface, forming a stem cell
148 population that go through several rounds of asymmetric divisions to produce cells that
149 differentiate either into pavement cells or stomata (Andriankaja et al., 2012). The identity of
150 these meristemoid cells are determined by a set of key regulators, such as SCPEECHLESS,
151 but can also be visually recognised by their characteristic round or square shape and a small
152 size of cells below the stomata guard cells, specifically less than $100 \mu\text{m}^2$ (Dong et al., 2009).
153 The temporal and spatial regulation of the cell cycle arrest front in the cell populations
154 originating from protodermal cells or meristemoids are different, but the underlying
155 molecular mechanisms are hitherto unknown (White, 2006).

156 We investigated how E2FB, which is considered to be an activator of cell proliferation, is
157 regulated by RBR interaction to underpin cell proliferation, exit to differentiation, and
158 establishment of quiescence during leaf development. Combined, our biochemical and
159 genetic analyses suggest that E2FB regulates organ development as a corepressor complex
160 with RBR.

161 **Results**

162 **Elevated E2FB level inhibits cell proliferation in association with RBR at early stages of**
163 **leaf development, whereas it perturbs the establishment of quiescence at later leaf**
164 **developmental stages when RBR levels decline**

165 To follow E2FB protein level in its native context during leaf development, we generated
166 Arabidopsis plants carrying the genomic region of *E2FB* under the control of its own
167 promoter and tagged its C-terminus with 3xVenus YFP, a modified yellow fluorescence
168 protein (pgE2FB-3xvYFP). In young leaves at six days after germination (6 DAG), the
169 E2FB-3xvYFP signal was detected in the nuclei both in the proliferating protodermal and
170 meristemoid cells (Figure 1A, 6 DAG). Interestingly, at a later stage of leaf development, the
171 E2FB-3xvYFP remained present in fully developed stomata as well as in lobbed
172 differentiated pavement cells and vascular cells with characteristic elongated nuclei close to
173 the cell wall (Figure 1A, 10 DAG). By comparing the E2FB-3xvYFP distribution with the
174 localisation of E2FA-3xvYFP and RBR-GFP (Magyar et al., 2012), we found that the E2FA-
175 3xvYFP was largely restricted to proliferating epidermal cells and was not detectable in fully
176 differentiated stomata (Supplemental Figure S1A and B). The RBR-GFP signal was present
177 in the meristemoids and in the proliferating and also in the differentiated pavement cells
178 (Supplemental Figure S1C). RBR was also detectable in fully differentiated stomata,
179 although at lower level (Matos et al., 2014).

180 To reduce a possible effect of 3xvYFP on the protein function, we also generated
181 transgenic Arabidopsis lines with a single GFP tag (pgE2FB-GFP), and showed that the
182 localisation of both E2FA-GFP and E2FB-GFP was comparable to that observed for E2FA-
183 3xvYFP and E2FB-3xvYFP in the different epidermal cell types (Supplemental Figure S1A
184 to F). Although *E2FB-GFP* expression was driven by the *E2FB* regulatory region, different
185 expression levels of *E2FB-GFP* were identified among the 36 independent transformants
186 (low, medium, and high; pgE2FB-GFP lines 61, 93, and 72, respectively, Supplemental
187 Figure S2A). Despite the difference in the levels, the temporal *E2FB-GFP* expression
188 followed the same declining pattern with leaf development as endogenous *E2FB* in the wild-
189 type (WT) control (Supplemental Figure S2B). The GFP-tagged E2FB was functional in
190 respect to its ability to interact with RBR as well as to dimerise with and to stabilise DPA and
191 DPB proteins (Supplemental Figure S2C to E). Its interaction with RBR protein was also
192 regulated as expected; it did not associate with the phosphorylated RBR form (Supplemental
193 Figure S2C).

194 Plants of pgE2FB-GFP line 72, with high *E2FB-GFP* expression driven by the *E2FB*
195 promoter, showed reduced growth habit compared to the WT both at seedling stage and as a
196 full-grown plant. As Figure 1B illustrates, the leaf area in pgE2FB-GFP line 72 was smaller

197 than WT. To investigate the cellular basis underlying the growth retardation, we imaged the
198 epidermal layer of the first leaf pair and quantified the leaf area, total cell number, stomata
199 number, cell size, and cell shape at three equal sections of the base, middle, and tip
200 (Supplemental Table S1-2). We took samples from pgE2FB-GFP lines 72 and 93 at two
201 developmental time points, representing young leaf with abundant cell proliferation (8 DAG)
202 and older leaf when the majority of cells undergo expansion growth (12 DAG, Supplemental
203 Figure S3 and Figure 1D). Surprisingly, this analysis revealed significantly fewer cells in
204 pgE2FB-GFP lines 72 and 93 compared to WT at 8 DAG, whereas this difference became
205 lower at 12 DAG (Figure 1D; Supplemental Table S1-2). In parallel, flow cytometry analysis
206 of DNA content showed an accumulation of 2C nuclei, representing G1 phase in pgE2FB-
207 GFP lines 72 and 93 at an early developmental stage (8 DAG) of the first leaf pair in
208 comparison to the WT, which also indicates a block in cell proliferation (Supplemental
209 Figure S3C). We also observed a shift towards larger cell size in pgE2FB-GFP line 72
210 compared to WT at 8 DAG (Supplemental Table S1, Supplemental Figure S3B). However, in
211 spite of the enlarged cell size, the entry into endoreduplication was delayed in both pgE2FB-
212 GFP lines 72 and 93 compared to WT, as shown by the reduced 8C nuclei in the first leaf pair
213 at 12 and 15 DAG (Supplemental Figure S3C). Ploidy level of the cotyledons was also
214 behind that of the WT in pgE2FB-GFP line 72, indicated by the reduced 16C and the
215 complete lack of 32C nuclear DNA content (Supplemental Figure S3D). In agreement with
216 this, the circularity index of epidermal cells was higher in pgE2FB-GFP lines than the
217 corresponding WT, suggesting that cells with elevated E2FB level are more round and thus
218 have delayed cell shape differentiation (Supplemental Table S1-2).

219 At 12 DAG, the majority of WT epidermal cells exited the cell cycle as indicated by
220 their elongated and lobbed outline. In pgE2FB-GFP line 72, we observed numerous straight
221 and less pronounced cell walls in these puzzle-shaped pavement cells, especially in cells
222 located further towards the leaf-tip area (Figure 1C, Supplemental Table S1-2, Supplemental
223 Figure S3A). The formation of a new division plane across the differentiated pavement cells
224 was even more frequent and pronounced on the cotyledon surface of pgE2FB-GFP line 72
225 (Supplemental Figure S3E). Some of these elongated pavement cells contained more than a
226 single straight cell wall. Similar divisions of enlarged pavement cells have been previously
227 reported in WT *Arabidopsis* leaves (Asl et al., 2011), but the frequency of these divisions
228 were dramatically increased in pgE2FB-GFP line 72 (Supplemental Table S1-2). In
229 agreement, in pgE2FB-GFP line 72, the proportion of middle-sized cells ($\leq 300\text{--}1000 \mu\text{m}^2$)

230 was elevated at 12 DAG at the expense of the number of larger cells (3000–6000 μm^2) as
231 compared to the WT (Supplemental Figure S3B).

232 To gain insights into the molecular mechanism leading to the altered cell proliferation
233 when E2FB level is elevated during leaf development, we first determined the expression
234 levels of the S-phase related *ORIGIN RECOGNITION COMPLEX 2 (ORC2)* and the mitotic
235 *CYCLIN-DEPENDENT KINASE B1;1 (CDKB1;1)*. In pgE2FB-GFP line 72, the expression
236 levels of *ORC2* and *CDKB1;1* were comparable to that in WT in young leaves (8 DAG,
237 Figure 2A). At 10 and 12 DAG, the expression of *ORC2* and *CDKB1;1* declined in WT,
238 where expression of these genes in pgE2FB-GFP line 72 remained elevated (Figure 2A). The
239 transcription of *CYCD3;1* and *RBR* also increased in pgE2FB-GFP line 72, most strikingly at
240 the time point of 10 DAG when expression of these genes in WT was significantly reduced
241 control (Figure 2A). The sustained expression of these cell cycle genes correlated well with
242 the division of enlarged pavement cells.

243 To understand how E2FB activity is regulated during leaf development, we studied
244 both RBR and its phosphorylation level and the interaction between E2FB and RBR. For this,
245 we utilised the human phosphospecific Rb^{S807/811} antibody that was shown to recognize the
246 conserved phosphorylation site of RBR proteins in multiple plant species, specifically at the
247 911 Serine position in Arabidopsis (P-RBR^{S911}, Abraham et al., 2011; Magyar et al., 2012;
248 Wang et al., 2014). In the WT, both RBR and E2FB protein levels, as well as RBR
249 phosphorylation, were highest at the early stage of leaf development (8 DAG) and displayed
250 a gradual decline afterwards when cells exited proliferation (10–12 DAG, Figure 2B and 2C).
251 By comparing RBR protein and phosphorylation levels in pgE2FB-GFP lines 93 and 72 to
252 that in the WT, we observed clear differences in their kinetics (Figure 2B). The endogenous
253 RBR level was highly elevated throughout the studied developmental stages in both pgE2FB-
254 GFP transgenic lines, indicating a regulatory loop to counteract the excess E2FB level
255 (Figure 2B and 2C). However, whereas RBR phosphorylation remained high at all studied
256 time points in pgE2FB-GFP line 72, it declined in pgE2FB-GFP line 93 to a level similar to
257 WT, indicating that RBR is more active as a repressor in pgE2FB-GFP line 93 than in
258 pgE2FB-GFP line 72 (Figure 2B, quantification in Supplemental Figure S4A and B). In
259 agreement, a considerably greater number of divisions were observed in differentiated
260 epidermal cells at 12 DAG in pgE2FB-GFP line 72 than in pgE2FB-GFP line 93
261 (Supplemental Table S2).

262 Next, we compared complex formation between E2FB-GFP and RBR proteins in
263 pgE2FB-GFP lines 93 and 72 (Figure 2C for inputs and 2D for co-IP). Immunoprecipitation
264 of E2FB-GFP showed that the majority of RBR protein was in complex with E2FB-GFP
265 fusion protein throughout leaf development and that the E2FB-RBR complex was the most
266 abundant in young leaves of both pgE2FB-GFP lines, providing an explanation why cell
267 number was decreased in the leaves of these lines (Figure 2D). The level of E2FB and RBR
268 proteins decreased as leaf development progressed, much more in pgE2FB-GFP line 93 than
269 in line 72 (Figure 2C, quantification in Supplemental Figure S4C and D), whereas the level of
270 E2FB-associated RBR was comparable between the pgE2FB-GFP lines (Figure 2D, for
271 quantification see Supplemental Figure S4E). Based on these data, we concluded that more
272 RBR-bound E2FB-GFP is present in pgE2FB-GFP line 93 than in line 72, whereas RBR-free
273 E2FB might be more prevalent in pgE2FB-GFP line 72 and consequently could promote cell
274 proliferation in lobed differentiated leaf pavement cells.

275 In summary, in young leaves, elevated E2FB level together with RBR present in
276 abundance represses rather than activates cell proliferation. The cellular and molecular data
277 indicate that excess E2FB can only be liberated from RBR repression at later developmental
278 stages when their levels decline, which leads to extra cell divisions in lobed pavement cells.

279 **The *e2fb* mutant has increased number of cells in developing leaves**

280 To investigate the effect of E2FB loss-of-function during leaf development, we analysed two
281 *e2fb* T-DNA insertion mutant alleles, *e2fb-1* (SALK_103138) and *e2fb-2* (SALK_120959)
282 (Berckmans et al., 2011; Kobayashi et al., 2015). The T-DNA insertions in these mutants are
283 located just behind and within the E2FB dimerization domain, respectively (Supplemental
284 Figure S5A). Based on the position of the T-DNA insertion, it is likely that *e2fb-2* is a null
285 mutant as it lacks the dimerization domain required to form a complex with DP proteins,
286 which is a prerequisite for E2Fs to bind to target promoters. Although no full-length E2FB
287 protein could be detected in either of these mutants (Supplemental Figure S5B; and for *e2fb-2*
288 see Berckmans et al., 2011), the size and morphology of both *e2fb-1* and *e2fb-2* seedlings
289 were largely comparable to WT; however, the area of the first leaf pair was moderately, but
290 significantly, larger than that in WT at 8 DAG and 12 DAG (Supplemental Figure S5C, and
291 Supplemental Table S1-2). In young leaves (8 DAG), the cell number in *e2fb* mutants was
292 comparable to WT, but cells were found to be enlarged in size (Supplemental Table S1).
293 Flow cytometry analysis revealed that some *e2fb* mutant leaf cells entered prematurely into

294 the endoreduplication cycle (Supplemental Figure S5D), thus suggesting that certain cells exit
295 cell proliferation earlier. By contrast, at the later developmental stage of 12 DAG, the number
296 of leaf epidermal cells in both *e2fb* mutants was significantly increased in comparison to WT
297 (Figure 3A and Supplemental Table S1-2). By introducing pgE2FB-GFP into the *e2fb-2*
298 mutant background, we could restore *e2fb* leaf epidermis cell number close to that of WT,
299 providing evidence of functional complementation (Figure 3A, and Supplemental Table S1-
300 2).

301 It is known that cells with meristemoid identity have a characteristic round or square
302 shape and a small cell size below the stomata guard cells that is less than $100\ \mu\text{m}^2$ (Dong et
303 al., 2009). We measured these cell types on the leaf epidermis at 12 DAG and found them to
304 be distributed below $60\ \mu\text{m}^2$. To reveal whether the increased cell number may result from
305 the overproliferation of meristemoids, we counted cells smaller than $60\ \mu\text{m}^2$. We indeed
306 found a much larger increase in both *e2fb* mutants within this cell population (Figure 3B). In
307 agreement, the total number of fully developed stomata also increased in the *e2fb* mutant
308 lines (Supplemental Table S1-2). These phenotypes were also complemented by expressing
309 E2FB-GFP in the *e2fb-2* mutant (Figure 3B), indicating that E2FB represses the proliferation
310 of leaf meristemoid cells. The E2FB-GFP protein accumulated to a much higher level in the
311 pgE2FB-GFP-complemented *e2fb-2* lines than that of endogenous E2FB protein in WT,
312 which explains why there was overcompensation (Figure 3D).

313 To study the impact of *e2fb* mutation on the expression of E2F target genes, we
314 selected the S-phase-specific genes *ORC2* and *MINICHROMOSOME MAINTENANCE*
315 *COMPLEX COMPONENT 3 (MCM3)*, the mitotic *CDKB1;1* and *CYCLIN A2;3 (CYCA2;3)*,
316 and the two mitosis upstream regulators *CYCD3;1* and *RBR*. The expression levels of all
317 these genes were reduced in the *e2fb* mutants, especially in young leaves (8 DAG). The
318 reduction was stronger in the null-mutant *e2fb-2* than in *e2fb-1* (Figure 3C). We also
319 investigated how the expression levels of the other two *E2F* genes were affected in the *e2fb*
320 mutants. The expression of *E2FA* did not change, whereas the *E2FC* transcript level showed
321 a slight elevation from 10 DAG onwards (Supplemental Figure S5E).

322 To gather further evidence that the mitotic *CDKB1;1*, *CYCD3;1*, and *RBR* genes are
323 directly regulated through the binding of E2FB to their promoters, we performed chromatin
324 immunoprecipitation (ChIP) experiments using the *e2fb-2* mutant complemented with the
325 pgE2FB-GFP construct. There was a significant enrichment of E2FB-GFP protein at the

326 promoter of these genes, specifically in the regions where consensus E2F binding elements
327 were predicted (Figure 4A and B).

328 These results show that whereas E2FB is required for the full activation of cell cycle
329 target genes at early stages of leaf development, its absence does not result in compromised
330 cell proliferation. On the contrary, E2FB has a prevalent importance to inhibit cell
331 proliferation, though at a later leaf developmental stage. This effect is most pronounced in
332 cells with a small size that likely belong to the stomata meristemoid lineage.

333 **Co-overexpression of *E2FB* with its dimerization partner *DPA* does not lead to** 334 **hyperproliferation in developing leaves**

335 Co-overexpression of *E2FB* but not *E2FA* with the dimerization partner *DPA* was shown to
336 overcome the requirement of the phytohormone auxin to promote cell proliferation in
337 cultured BY2 tobacco cells (Magyar et al., 2005). In animals, the expression of activator
338 E2Fs is increased in most cancer types and thought to be responsible for uncontrolled
339 cancerous cell proliferations (Chen et al., 2009). To determine whether such overexpression
340 causes cell overproliferation in plants, we studied the Arabidopsis line p35S::HA-E2FB/*DPA*
341 (*E2FB/DPA*^{OE}), which overexpresses both *E2FB* and *DPA* (De Veylder et al., 2002; Magyar
342 et al., 2012; Horvath et al., 2017). In contrast to the expected deregulation of cell proliferation
343 and disruption of plant development, we did not observe tumorous growth. Leaf initiation
344 proceeded normally; however, *E2FB/DPA*^{OE} seedlings were smaller and the total leaf area
345 was reduced to half of that of WT (Figure 5A).

346 To study the cellular basis behind the retarded leaf growth, we imaged the epidermal
347 cell layer of the *E2FB/DPA*^{OE} line at 8 and 12 DAG (Figure 5B) and measured cell
348 parameters (Supplemental Table S1-2). At 8 DAG we observed predominantly small-sized
349 and polygonal shaped cells across the entire leaf surface, but the total calculated cell number
350 was less than in WT (Figure 5B and Supplemental Figure S6A and S6D), indicating that both
351 cell proliferation and cell enlargement are inhibited at early stages of leaf development by the
352 overexpression of E2FB together with *DPA*. By contrast, at 12 DAG the calculated leaf
353 epidermal cell number of *E2FB/DPA*^{OE} was comparable to WT, whereas cell size remained
354 smaller (Figure 5B, 12 DAG, Supplemental Table 2, Supplemental Figure S6D), suggesting
355 that the transition from proliferation to cell elongation is delayed. The reduced stomatal index
356 and the less complex shape of pavement cells (circularity index) at both time points also

357 indicated an inhibition of stomata as well as pavement cell differentiation (Supplemental
358 Table S1-2). E2FB/DPA^{OE} seedlings also displayed down-curling cotyledons (Figure 5A). In
359 WT cotyledons at 6 DAG, cell proliferation ceases and all pavement and stomata cells appear
360 differentiated. By contrast, there were a large number of small cells in the cotyledons of
361 E2FB/DPA^{OE} seedlings (Supplemental Figure S6B).

362 In E2FB/DPA^{OE} seedlings, the level of *E2FB* expression increased from 50 to 100
363 fold that of the WT level throughout leaf development (Figure 5C). By contrast, the
364 accumulation of E2FB protein did not match the constitutive overexpression of the *E2FB*
365 transcript; its level was highly elevated at the earliest time point only (9 DAG) and showed
366 diminished accumulation reaching levels comparable to the endogenous E2FB protein at later
367 timepoints (Figure 5D). The DPA protein level showed the same kinetics as E2FB (Figure
368 5D), suggesting their developmental co-regulation at the protein level. The level of the
369 mitotic CDKB1;1 protein was also high in young leaves, but diminished towards the 16 DAG
370 timepoint (Figure 5D). The co-regulation of E2FB and DPA protein with the same kinetics
371 was also observed in cotyledons (Supplemental Figure S6C).

372 Surprisingly, there was no excess of cell proliferation in the E2FB/DPA^{OE} line, and so
373 we looked to see whether there was any deregulation of E2F target genes in this line. We
374 analyzed the expression of two S-phase specific genes, *ORC2* and *MCM3*, and the mitotic
375 *CDKB1;1* (Figure 6A). These E2F target genes were greatly upregulated throughout leaf
376 development in the E2FB/DPA^{OE} line, although they declined in parallel with the diminishing
377 E2FB and DPA protein levels as leaf development progressed (Figure 6A-B and Figure 5D).
378 Two other cell cycle genes were tested, namely the CDK inhibitor *KIP-RELATED PROTEIN*
379 *4 (KRP4)* and *CYCLINA3;1 (CYCA3;1)*, which were also upregulated but not to the same
380 extent and their upregulated expression was not observed at every time point (Supplemental
381 Figure S6E). Expression of the upstream positive and negative regulators of *E2FB*, *CYCD3;1*
382 and *RBR*, respectively, were also upregulated in the E2FB/DPA^{OE} line (Figure 6A),
383 indicating the presence of a regulatory feedback loop. In accordance, we also found an
384 elevated RBR protein level and RBR phosphorylation (P-RBR^{S911}) in E2FB/DPA^{OE} leaves
385 compared to WT (Figure 6B, for quantification see Supplemental Figure S6F and G). RBR
386 was also strongly upregulated in E2FB/DPA^{OE} cotyledons (Supplemental Figure S6C).

387 To explore how the overexpression of *E2FB/DPA* and the consequent change in RBR
388 level and its phosphorylation affected the amount of RBR-associated E2FB, we performed

389 co-immunoprecipitation experiments (Figure 6C and D). Utilising the HA-tag on E2FB in the
390 E2FB/DPA^{OE} line, we immunoprecipitated HA-E2FB from seedlings (7 DAG). As Figure 6C
391 shows, only a relatively small amount of DPA was associated with HA-E2FB, and RBR was
392 also not enriched in the complex. However, using the DPA antibody in young leaves (8
393 DAG), we detected a higher level of immunoprecipitated E2FB as well as RBR compared to
394 those levels observed in seedlings (Figure 6C and D). This shows that RBR effectively binds
395 to the overexpressed E2FB-DPA heterodimer in young leaves, which explains the repression
396 of cell proliferation. However, in some cells or at some cell cycle stages, active RBR-free
397 E2FB-DPA heterodimer must also be present to cause the high upregulation of E2F target
398 genes.

399 **RBR recruitment through E2FB is important to halt cell proliferation in developing** 400 **leaves**

401 To address how the function of E2FB is dependent on its ability to bind RBR, we constructed
402 a truncated E2FB where we deleted the C-terminal 84 amino-acid region containing the
403 conserved RBR-binding and the overlapping transactivation domains, as we previously did
404 for E2FA (Magyar et al., 2012), and co-overexpressed this HA-tagged E2FB^{ARBR} with DPA
405 (Supplemental Figure S7A), as we did for the full-length E2FA earlier. Two independent
406 HA-E2FB^{ARBR}/DPA lines (1 and 10) showed identical developmental abnormalities; their
407 growth was arrested both *in vitro* and on soil (Figure 7A, Supplemental Figure S7B-C). With
408 high frequency (10–15%), we observed abnormally developing seedlings that had three
409 cotyledons and missing or fused organs, indicating abnormal embryo development
410 (Supplemental Figure S7B). In the HA-E2FB^{ARBR}/DPA line, we observed clusters of small
411 cells on the leaf epidermis interspersed among large lobbed pavement cells (Figure 7B, and
412 Supplemental Figure S8A and F). Quantifying epidermal cell sizes over a developmental time
413 series (8, 10, and 12 DAG, Supplemental Figure S8B, and Supplemental Table S1-2) showed
414 that the ratio of small-sized cells ($\leq 300 \mu\text{m}^2$) diminished gradually in WT, but remained high
415 in both independent HA-E2FB^{ARBR}/DPA lines. On the other hand, large cells (1000–3000
416 μm^2) formed earlier in the HA-E2FB^{ARBR}/DPA lines than in WT, and at 8 DAG the large
417 cells were also more prominent in the middle and the tip region of the leaf (Supplemental
418 Figure S8C). In agreement, the total cell number in the leaf was also higher in the
419 E2FB^{ARBR}/DPA lines compared to WT at the later developmental stage of 12 DAG
420 (Supplemental Table S1-2). To reveal the proportion of possible stomata meristemoids

421 among the small cells that are prominent at the late leaf developmental stage of 12 DAG, we
422 quantified the number of cells with $\leq 60 \mu\text{m}^2$. This cell population showed an even larger
423 increase, specifically more than four-fold greater in the HA-E2FB^{ΔRBR}/DPA lines compared
424 to WT (Supplemental Figure S8D).

425 To reveal whether cell size relates to ploidy changes, we measured the DNA content
426 in the first leaf pairs of HA-E2FB^{ΔRBR}/DPA, but found no difference compared to WT
427 (Supplemental Figure S8E). Thus, the observed phenotypes of HA-E2FB^{ΔRBR}/DPA lines
428 were markedly different from what was observed previously for the HA-E2FA^{ΔRBR}/DPA line,
429 which showed a dramatically elevated extent of endoreduplication (Magyar et al., 2012).

430 To gather molecular evidence behind the sustained proliferation in the cell clusters
431 observed in the HA-E2FB^{ΔRBR}/DPA line, we determined CDK activity using p13^{Suc1} affinity
432 chromatography that pulls down both A- and B-type CDKs (Magyar et al., 2005). As
433 expected, CDK activity declined in WT, whereas it remained high throughout leaf
434 development in the HA-E2FB^{ΔRBR}/DPA line (Figure 7C), further supporting the persistence
435 of cell proliferation in this line. To demonstrate that the C-terminally truncated E2FB cannot
436 bind RBR, we utilised transgenic lines where we tagged at the N-termini of both E2FA and
437 E2FB deletion constructs with GFP for efficient pull down (Figure 7D and see details in
438 Materials and Methods). By using these transgenic lines in co-immunoprecipitation
439 experiments, we confirmed that neither E2FA nor E2FB could pull RBR down in the absence
440 of the C-terminal RBR-binding domain, but both associated with the DPB protein (Figure
441 7D).

442 We also determined the expression of cell cycle E2F target genes (*ORC2*, *CDKB1;1*,
443 *CYCD3;1*, and *RBR*) in both HA-E2FB^{ΔRBR}/DPA lines during leaf development (Figure 7E).
444 The transcript levels of all examined genes were upregulated at 8 and 10 DAG compared to
445 WT (Figure 7E). Since HA-E2FB^{ΔRBR} lacks the transactivation domain, this upregulation is
446 likely due to the lack of RBR repression on these genes.

447 In summary, whereas the deletion of the RBR-binding domain in the HA-
448 E2FA^{ΔRBR}/DPA lines leads to dramatic over-endoreduplication (Magyar et al., 2012), the
449 same manipulation made to E2FB in HA-E2FB^{ΔRBR}/DPA lines results in overproliferation of
450 cell clusters during leaf development.

451 Discussion

452 Plant growth is centred on meristem activity, yet surprisingly little is known about how cell
453 proliferation is regulated at the molecular level in a developmental context. E2F transcription
454 factors are the prime candidates for regulating meristematic function in close association with
455 RBR. Previously, we showed that E2FA in complex with RBR is involved in meristem
456 maintenance (Magyar et al., 2012). E2FB was considered as a canonical transcriptional
457 activator, and indeed we found that its overexpression can activate the expression of cell
458 cycle genes, whereas *e2fb* mutations compromise expression of these same genes. However,
459 the cell proliferation outcome does not follow these molecular changes in the developing
460 leaves. On one hand, elevated or ectopic overexpression of E2FB (pgE2FB-GFP or
461 p35S:HA-E2FB/DPA) causes a decrease in total cell number rather than an increase. On the
462 other hand, the *e2fb* mutant lines produce more cells during leaf development in comparison
463 to the control WT. Furthermore, we demonstrated both biochemically and genetically that the
464 repressor function of E2FB on cell proliferation relies on the RBR association, which is
465 reinforced by autoregulatory loops.

466 In animal cells, Rb level and activity increases as cells exit proliferation and enter
467 differentiation (Zacksenhaus et al., 1996). By contrast, RBR in plants is most abundant in
468 meristematic cells, and its level diminishes as development proceeds (Borghini et al., 2010;
469 Magyar et al., 2012). Thus, RBR co-expresses with E2FA and E2FB in proliferating plant
470 cells and forms repressor complexes. Moreover, we found that elevated and ectopic
471 overexpression of E2FB leads to increased RBR level. This autoregulatory loop enforces the
472 repression, which ensures that cell proliferation is kept under control and thus increased
473 E2FB level does not lead to tumorous growth. RBR repression on cell proliferation through
474 inhibiting E2FB is suppressed by RBR phosphorylation, and E2FB positively regulates the
475 regulatory cyclin subunit (CYCD3;1) of the RBR-kinase (CDKA;1) as well. It is known that
476 Rb phosphorylation and thus repressor activity is cell-cycle regulated; dephosphorylated Rb
477 is active in G1 phase and as cells pass through the G1/S control point the
478 hyperphosphorylated Rb becomes inactive, leading to the expression of cell cycle genes
479 (Morgan, 2007). It is feasible that in plants the elevated E2FB and consequent RBR levels in
480 G1 leads to overabundance of E2FB-RBR repressor complex and thereby inhibition of cell
481 proliferation, whereas after cells pass through the control point, when RBR becomes
482 hyperphosphorylated, the overexpressed and now free E2FB hyperactivates cell cycle target

483 genes. A block in cell proliferation is consistent with increased 2C DNA content when E2FB
484 is elevated.

485 Both the protein levels of E2FB and RBR decline as leaf development proceeds.
486 During this transition phase from cell proliferation to differentiation, the E2FB-RBR complex
487 is important to exit cell proliferation and to establish quiescence. When E2FB escapes from
488 RBR repression after the transition phase, differentiated cells re-enter cell division, which is
489 the case when E2FB level is elevated with expression driven by its own promoter. When
490 E2FB is ectopically overexpressed together with DPA, these extra cell divisions of
491 differentiated pavement cells were not present. Instead, cells are arrested in an
492 undifferentiated state, as indicated by their small size without lobbed shape and decreased
493 number of stomata. This suggests that overexpression of E2FB together with DPA prevents
494 the transition from proliferation to differentiation. Thus, the ectopic co-overexpression of
495 E2FB with DPA or elevation of E2FB with expression driven by its own promoter have very
496 different consequences. In the first case, a large amount of E2FB-DPA heterodimer is present
497 that is still kept under control of RBR to inhibit both cell proliferation and differentiation,
498 leading to growth arrest. The destabilisation of E2FB and DPA during leaf development may
499 allow an escape mechanism from this block. By contrast, elevated E2FB with expression
500 driven by its own promoter can form heterodimers either with the endogenously available
501 DPA or DPB. It was suggested that the interaction of DPA with activator E2Fs stimulates
502 nuclear translocation and mediates a higher level of transactivation than interaction with DPB
503 (Kosugi and Ohashi, 2002). This might explain why there is less pronounced growth arrest
504 and cells can exit proliferation when the E2FB level is elevated on its own.

505 We show that E2FB is required and sufficient to restrain cell proliferation in
506 developing leaves by demonstrating that leaves produce fewer cells when *E2FB* is
507 overexpressed and more cells when it is mutated. We also show biochemically that E2FB has
508 strong affinity to associate with RBR in young leaves enriched with proliferating cells. To
509 provide further evidence that RBR acts through E2FB to inhibit cell proliferation, we deleted
510 the C-terminal RBR binding domain of E2FB and overexpressed this mutant form with DPA.
511 Indeed, we observed overproliferation of cells in developing leaves that strongly suggests that
512 the formation of RBR-E2FB repressor complex is important to control cell proliferation
513 during leaf development. Based on their small size and shape, proliferation in clusters, and
514 the increased number of fully developed stomata at a later stage, the cell overproliferation is

515 likely within the stomata meristemoid lineage, but this has to be confirmed by cell type
516 specific markers, such as the expression of *SPEECHLESS*. Because the C-terminal deletion
517 on E2FB also removed the transactivation domain, the overproliferation of meristemoids
518 must be a consequence of derepression from RBR control. The presence of meristemoid
519 overproliferation in two independent *e2fb* mutants strongly suggests that this phenotype is
520 E2FB specific.

521 RBR silencing was shown to upregulate the expression of *TOO MANY MOUTH*
522 (*TMM*), the key regulator of stomata meristemoid divisions, leading to their overproliferation
523 (Borghi et al., 2010). At later developmental stages in the stomata lineage, RBR silencing can
524 also interfere with the division arrest of the fully developed guard cells (Borghi et al., 2010;
525 Yang et al., 2014). We did not observe such phenotypes when the truncated E2FB was
526 overexpressed, suggesting that RBR does not regulate these later steps in stomata
527 differentiation through E2FB association, but likely through binding and repression of other
528 transcription factors, as it was shown in the case of FAMA (Xie et al., 2010). Interestingly,
529 SOL1 and SOL2, two Arabidopsis homologues of LIN54, a component with DNA binding
530 activity within the mammalian DREAM complex, were shown to regulate cell fate and
531 division in the stomatal lineage (Simmons et al., 2019). Both SOL1 and SOL2 were found to
532 be upregulated in the E2FA/DPA overexpression line, but only SOL2 was hyper-activated in
533 RBR-silenced RBR-RNAi plants and has the consensus E2F-binding element in its promoter
534 region (Borghi et al., 2010). Accordingly, the E2F-RBR pathway could regulate these
535 transcription factors, but whether these DREAM-related components function in complex
536 with E2Fs and RBR to control cell proliferation in the stomatal lineage is not yet known.

537 Using GFP-tagged constructs, we found important differences in the expression
538 pattern of these two E2Fs; E2FA is largely restricted to proliferating cells whereas E2FB and
539 RBR are also present in differentiated pavement and fully developed stomata guard cells. The
540 co-occurrence of E2FB but not E2FA with RBR in these differentiated cell types is consistent
541 with the idea that E2FB with RBR is required to repress cell proliferation and impose
542 quiescence to allow differentiation, whereas E2FA acts with RBR to maintain proliferation
543 competence (Magyar et al., 2012). E2FA and E2FB are also distinctly regulated by RBR;
544 excess sucrose or overexpression of *CYCD3;1* promotes E2FA-RBR interaction whereas
545 these factors disrupt E2FB-RBR interaction (Magyar et al., 2012). The distinct cellular
546 phenotypes upon the overexpression of C-terminally truncated dominant-negative forms of

547 E2FA or E2FB further underlines the difference in the mode of their action in relation to
548 RBR-repression and transactivation of target genes. The overexpression of E2FA^{ΔRBR}
549 resulted in over-endoreduplication due to the inability to repress the expression of
550 endoreduplication genes (Magyar et al., 2012), whereas E2FB^{ΔRBR} overexpression had no
551 effect on endoreduplication, but led to the early formation of large pavement cells and
552 clusters of small cells. The fact that overexpression of both the full-length and the truncated
553 forms of E2FA and E2FB have specific phenotypic outcomes suggest that they might have
554 distinct sets of target genes. In agreement, overexpression of E2FA and E2FC also caused
555 very different genes to be deregulated (de Jager et al., 2009).

556 The functional difference between E2FA and E2FB may rely on their interaction with
557 distinct sets of proteins. As we previously showed, E2FB and E2FC can associate with
558 proteins that are known to be conserved components of the so-called DREAM complex
559 (Kobayashi et al., 2015). By contrast, though E2FA can interact with RBR and DPs, none of
560 the DREAM components were found in complex with E2FA (Horvath et al., 2017). Both
561 E2FB and E2FC, as part of the DREAM complex, function to repress cell proliferation.
562 However, our results suggest that E2FB acts at an earlier stage during the transition from
563 proliferation to differentiation as well as in the immediate establishment of quiescence,
564 possibly as part of the activator MYB3R1/4 complex (Kobayashi et al., 2015), whereas E2FC
565 might be required at a later stage to permanently maintain the cell cycle repression (del Pozo
566 et al., 2006), as part of the repressor MYB3R1/3/5 complex (Kobayashi et al., 2015).

567 Plants are remarkably resistant to cancerous transformation, but this ability is poorly
568 understood (Doonan and Hunt, 1996). In animals, the activator E2Fs are found to be
569 increased in most cancer types and they contribute to the uncontrolled proliferations (Chen et
570 al., 2009). Here, we show that E2FB, the canonical activator E2F in Arabidopsis, could not
571 drive cancerous divisions even when its level was elevated fifty fold. A potential reason why
572 the large amount of E2FB does not activate tumorous growth is the direct activation of RBR
573 by E2FB and the accumulation of RBR/E2FB repressor complex in proliferating cells.
574 However, CYCD3;1 is also a direct target of E2FB leading to increased RBR
575 phosphorylation and inactivation of RBR repression. It is likely that the simultaneous
576 activation of positive and negative upstream regulators to E2FB is important to keep cell
577 proliferation under tight control in plant cells.

578 In summary, E2FB-RBR relays meristematic activities to differentiation through the
579 regulation of (1) cell cycle transitions by transcriptional activation of cell cycle genes, (2) cell
580 cycle exit and establishment of quiescence through the repression of cell cycle genes when
581 associated with RBR, and (3) stem cell amplifying divisions through an active repression
582 mechanism together with RBR (Figure 8). Plant growth is fundamentally determined by the
583 number of cells kept in proliferation in the meristem (Bogre et al., 2008). Meristem size is
584 sensitively responsive to environmental conditions and we suggest that the interconnected
585 action of the three E2Fs plays a central role in meristem activities, thus providing an entry
586 point to understand and manipulate the growth potential of plants and crops.

587 **Materials and Methods**

588 **Plant material and growth conditions**

589 *Arabidopsis thaliana* ecotype Columbia wild-type (WT) and transgenic seeds were sterilized
590 in commercial bleach, re-suspended in sterile water, and cold-treated at 4°C in darkness for 2
591 days (Clough and Bent, 1998). Unless otherwise stated, plants were grown under a 16-h
592 light/8-h dark photoperiod at 22°C *in vitro* on half-strength germination medium (1/2GM)
593 with 100 $\mu\text{Em}^{-2} \text{s}^{-1}$ light intensity or on soil mixture of decomposed raised bog peat
594 (Plantobalt; Plantaflor Humus Verkaufs-GmbH) under long-day conditions (16-h light/8-h
595 dark) with 100 $\mu\text{Em}^{-2} \text{s}^{-1}$ light intensity. The cotyledons and the first leaf pairs of WT or the
596 transgenic *Arabidopsis* lines (p35S:HA-E2FB/DPA, pgE2FB-GFP, and p35S:HA-
597 E2FB^{ARBR}/DPA) grown *in vitro* were harvested 8–15 DAG, flash frozen, and stored at -80°C.
598 The T-DNA insertion mutants of E2FB were previously reported (*e2fb-1* - SALK_103138
599 and *e2fb-2* - SALK_120959; Berckmans et al., 2011; Heyman et al., 2011; Horvath et al.,
600 2017).

601 **Plasmid construction and generation of transgenic *Arabidopsis* plants**

602 The construct of the pE2FB:gE2FB-GFP (pgE2FB-GFP) and the pE2FA:gE2FA-GFP
603 (pgE2FA-GFP) translational fusion has been described before (Berckmans et al., 2011;
604 Magyar et al., 2012). Using the pgE2FB-GFP construct, transgenic *Arabidopsis* lines were
605 generated by *Agrobacterium*-mediated transformation in the WT (Col-0) background and 36
606 independent T1 *Arabidopsis* lines were identified on selection medium containing
607 norflurazon. The pgE2FB-GFP construct was also introduced into the *e2fb-2* mutant by
608 *Agrobacterium*-mediated transformation and homozygous T2 lines were generated
609 afterwards. The genomic sequence of E2FB or E2FA was also fused in frame with triple
610 Venus YFP (3xvYFP) in a pGreenII-based pGII0125 destination vector (Galinha et al., 2007)
611 by using the Invitrogen 3way Gateway System (Invitrogen, USA). The previously described
612 HA epitope-tagged full length E2FB and its C-terminal deletion mutant form (HA-E2FB^{ARBR})
613 missing an 84 amino acid-long region containing the conserved RBR-binding motif (Magyar
614 et al., 2000) were placed under the control of the constitutive cauliflower mosaic virus 35S
615 promoter in the Gateway vector pK7WG2 (Karimi et al., 2002). These constructs were
616 introduced into the previously established p35S:DPA transgenic *Arabidopsis* line (De
617 Veylder et al., 2002) using the floral-dip method for *Agrobacterium*-mediated transformation

618 as described (Zhang et al., 2006). Thirteen p35S:HA-E2FB/DPA co-overexpression
619 transgenic T1 lines were selected based on the presence of the appropriate antibiotic
620 resistance (kanamycin). A strong HA-E2FB expressing single copy T-DNA insertion line was
621 identified and homozygous T2 segregation was selected on kanamycin-containing medium.
622 Twelve p35S:HA-E2FB^{ΔRBR}/DPA primary transgenic lines were identified and two
623 homozygous T2 segregations (named as 1/10 and 10/X) were selected on medium containing
624 kanamycin for further studies. We generated the GFP-tagged version of E2FA^{ΔRBR} and
625 E2FB^{ΔRBR} where we cloned the C-terminal deleted version (missing the entire transactivation
626 domains until the Marked box region; deletion of 135- and 160 amino acid-long regions from
627 the C-terminus of E2FA and E2FB, respectively) into the pK7WGF2 gateway vector adding
628 the GFP tag to the N-terminal position. In each case, 15 independent single copy T-DNA
629 insertion lines were identified on kanamycin-containing medium.

630 **RNA extraction and reverse transcription quantitative PCR (RT-qPCR)**

631 RNA was extracted from leaf samples using the RNeasy Plant Mini Kit (Qiagen, UK). cDNA
632 was synthesized using 1 μg of RNA using the QuantiTect Reverse Transcription Kit
633 (Qiagen). Reverse transcription quantitative PCR (RT-qPCR) in the presence of SYBR Green
634 was carried out using a BioScript PCR kit (Bioline, UK) according to the manufacturer's
635 instructions in a Rotor-Gene 6000 apparatus (Corbert Life Science, Australia). All the data
636 was normalized to housekeeping genes (*ACTIN* and/or *UBIQUITIN*) and the calculated
637 efficiency was added to the analysis. Primer sequences are summarised in Supplemental.
638 Table S3. All reactions were carried out in triplicate.

639

640 **Image and flow cytometry analysis, determining cellular parameters of leaf samples**

641 To visualize the leaf or cotyledon epidermis, a gel cast was made of the leaf surface,
642 specifically the adaxial side of the first leaf pair, which was then observed under a DIC light
643 microscope Nikon Optiphot 2 as described (Horiguchi et al., 2006).

644 First true leaf pairs of WT and of various transgenic lines were dissected from seedlings at 8
645 or 12 DAG. Leaves were stained with propidium iodide (PI, 20 mg/ml) and images on the
646 abaxial side of three different zones (the basal, middle and tip part) of the leaf were taken and

647 analyzed by confocal laser microscopy (Leica SP5, Germany). Across the three zones,
648 approximately 600 cells were counted and measured per leaf sample, $n \geq 3$ were studied for
649 each transgenic line and the control using the Image J software. Average cell size was
650 calculated and the total cell number was extrapolated to the whole leaf according to
651 previously described methods (Asl et al., 2011). The stomata number and stomatal index was
652 calculated in a similar way. For determining the circularity of epidermal cells by using Image
653 J software, guard cells were extracted (Andriankaja et al., 2012). To visualize the
654 distributions of the cell area, only non-guard epidermal cells from the three zones were
655 pooled together and used for calculation at a given time point, unless described otherwise
656 (Asl et al., 2011). The number of elongated pavement cells with newly formed cell wall
657 (described as extra cell division) was counted in all three zones and extrapolated to the whole
658 leaf.

659 For flow cytometry measurements, the first leaf pairs were collected and chopped with razor
660 blades in nuclei extraction buffer and stained with DAPI as described before (Magyar et al.,
661 2005). Flow cytometry data were obtained using a Partec PAS2 Particle Analysing system
662 (Partec, Germany).

663

664 **Immunoprecipitation, immunoblotting, and kinase assays**

665 Immunoprecipitation (IP) and immunoblotting assays were carried out as described
666 (Henriques et al., 2010). Briefly, total proteins were extracted from dissected leaves or
667 seedlings in extraction buffer (25 mM Tris-HCl pH 7.5, 75 mM NaCl, 15 mM MgCl₂, 15 mM
668 EGTA, 15 mM p-nitrophenylphosphate, 60 mM β -glycerophosphate, 1 mM DTT, 0.1 %
669 IgePal CA630, 0.5 mM NaF, 1 mM phenylmethylsulfonyl fluoride, 1 \times protease inhibitor
670 cocktail-Sigma P9599). Equal amount of proteins were loaded to SDS-Polyacrylamide
671 (PAGE) gel (10% or 12%), and proteins were transferred onto polyvinylidene difluoride
672 (Millipore, Bedford) membranes. The membranes were blocked in 5% (w/v) milk powder
673 with 0.05% (v/v) Tween-20 in TBS (25mM Tris-Cl, pH 8.0, 150mM NaCl; TBST) buffer for
674 one hour at room temperature. The membrane was incubated with 5% (w/v) milk-powder
675 TBST containing the primary antibodies and agitated overnight at 4⁰C. Primary antibodies
676 used in immunoblotting experiments: chicken anti-RBR antibody (1:2000 dilution, Agrisera,
677 Sweden), mouse monoclonal anti-PSTAIRES (1:40000 dilution, CDKA;1 specific; Sigma),

678 rabbit polyclonal antibody anti-CDKB1;1 (1:2000 dilution; Magyar et al., 2005), anti-
679 phospho-specific Rb (Ser807/811) rabbit polyclonal antibody (1:500 dilution, Cell Signaling
680 Tech), anti-E2FB polyclonal rabbit antibody (1:400 dilution, Magyar et al., 2005). After the
681 primary antibody reaction, the membrane was washed three times with TBST, and incubated
682 with the appropriate secondary antibody conjugated with horseradish peroxidase (HRP) for
683 another hour at room temperature, followed by three washing steps (TBST) and afterwards
684 chemiluminescence substrate was applied according to the manufacturer description
685 (SuperSignal West Pico Plus – Thermo Scientific, USA or Immobilon Western HRP –
686 Millipore, USA). For immunoprecipitation equal amount of protein samples (between 500–
687 800 µg) in extraction buffer (see above) were incubated with antibodies or GFP-trap
688 magnetic agarose beads (8–10 µL – ChromoTek, Germany) for 40 minutes to 1 hour at 4°C.
689 The following antibodies have been used in co-IP experiments: anti-DPA (Magyar et al.,
690 2005) and anti-DPB (Umbrasaitė et al., 2010), and anti-GFP monoclonal mouse antibody
691 (Roche) or GFP-Trap coupled to magnetic agarose beads (ChromoTek). Protein A or protein
692 G-Sepharose were used to pulldown polyclonal or monoclonal antibodies, respectively, and
693 then the beads were washed three times with extraction buffer and proteins were eluted by
694 adding SDS-sample buffer followed by 5 minutes boiling. Eluted proteins were loaded on
695 SDS-PAGE (10% or 12%) and after protein gel-electrophoresis they were immunoblotted as
696 described above.

697 The kinase assay was carried out as described earlier (Magyar et al., 1997). Briefly, total
698 proteins were extracted from frozen leaf samples harvested 8–15 DAG and equal protein
699 amounts were incubated with p13^{Suc1}-Sepharose beads for an hour at 4°C on rotary shaker.
700 Kinase reaction was initiated by the addition of 1 mg/mL histone H1 substrate and 2.5 µCi of
701 γ -³²P-ATP.

702 **Chromatin immunoprecipitations (ChIP)**

703 Chromatin immunoprecipitation (ChIP) assay was carried out as described previously (Saleh
704 et al., 2008). Four grams of E2FB-GFP-, E2FA-GFP-, and GFP-expressing seedlings, the
705 latter from a 35S:GFP line, were crosslinked with 1% (w/v) formaldehyde solution at 6 DAG.
706 Chromatin was precipitated using anti-GFP polyclonal rabbit antibody (Invitrogen) and were
707 collected with salmon sperm DNA/protein A-agarose (Sigma). The purified DNA was used
708 in RT-qPCR reactions to amplify promoter regions with specific primers listed in

709 Supplemental Table 3. Fold DNA enrichment was calculated by dividing the antibody
710 immunoprecipitation signals with the no-antibody signals.

711 Accession numbers

712 Sequence data from this article can be found in the GenBank/EMBL data libraries under
713 accession numbers: ATE2FB, AT5G22220; ATE2FA, AT3G36010; ATE2FC, AT1G47870;
714 ATDPA, AT5G02470; ATDPB, AT5G03415; ATRBR, AT3G12280; ATCDKA;1,
715 AT3G48750, ATCDKB1;1, AT5G54180; ATCYCD3;1, AT4G34160; ATCYCA2;3,
716 AT1G15570; ATCYCA3;1, AT5G34080; KRP4, AT2G32710; MCM3, AT5G46280; ORC2,
717 AT2G37560.

718

719 Supplemental Data

720 **Supplemental Figure S1.** E2FB and RBR, but not E2FA, are present in differentiated
721 pavement and fully developed stomata guard cells.

722 **Supplemental Figure S2.** The E2FB-GFP protein could make complex with DPs, and the
723 non-phosphorylated form of RBR, with these well-known, major interactors of E2FB.

724 **Supplemental Figure S3.** Elevated expression of *E2FB* with expression driven by its own
725 promoter inhibits cell proliferation in young leaves and disturbs quiescence in older leaves.

726 **Supplemental Figure S4.** E2FB-GFP binds less RBR in older leaves of pgE2FB-GFP line
727 72 than in line 93.

728 **Supplemental Figure S5.** Lack of E2FB function prematurely switches mitosis to endocycle.

729 **Supplemental Figure S6.** Elevated HA-E2FB/DPA heterodimer stimulates the accumulation
730 of RBR and its phosphorylated form, RBR^{S911}.

731 **Supplemental Figure S7.** Mutant E2FB protein (HA-E2FB^{ΔRBR}) in conjunction with DPA
732 causes drastic phenotypic changes during development.

733 **Supplemental Figure S8.** Expression of HA-E2FB^{ΔRBR}/DPA hyper-activates cell
734 proliferation of meristemoid cells.

735 **Supplemental Table S1.** Cellular parameters quantified from the first leaf pair of WT and
736 E2FB-related transgenic lines of leaf development at 8 DAG.

737 **Supplemental Table S2.** Cellular parameters quantified from the first leaf pair of WT and
738 E2FB-related transgenic lines of leaf development at 12 DAG.

739 **Supplemental Table S3.** List of primers and their sequences used for RT-qPCR analysis and
740 in ChIP assays.

741

742

743 **Acknowledgements**

744 We thank Ferhan Ayaydin (BRC Szeged, Hungary) for helping in microscopy, and Anita
745 Kovács (BRC Szeged, Hungary) for her assistance in plant work. .E.Ő., A.P-Sz, T.L., E.M.
746 and Z.M. were supported by the Hungarian Scientific Research Fund (OTKA K-105816) and
747 by the Ministry for National Economy (Hungary, GINOP-2.3.2-15-2016-00001). T.L. was
748 funded by the Young Scientist Fellowship of the Hungarian Academy of Sciences, A.P-Sz.
749 was supported by the GINOP-2.3.2-15-2016-00032. Cs.P and B.M.H. were funded by the
750 Marie Curie IEF fellowships (FP7-PEOPLE-2012-IEF.330713 and FP7-PEOPLE-2012-
751 IEF.330789, respectively). Cs.P. and L.B were funded by the BBSRC-NSF grant
752 (BB/M025047/1). The funders had no role in the design of the study, data collection and
753 analysis, decision to publish, or preparation of the manuscript.

754 **Conflict of interest**

755 The authors declare that they have no conflict of interest.

756

757 **Figure Legends**

758

759 **Figure 1. Elevated E2FB level in its own expression domain inhibits cell proliferation in**
760 **young leaves and disturbs quiescence in older leaves.**

761

762 (A) Representative confocal laser scanning microscopy (CM) images of the abaxial leaf
763 surface from the first leaf pair of the transgenic line pgE2FB-3xvYFP at 6 and 10 days after
764 germination (DAG; top panels), and localisation in the epidermis and vascular tissues of the
765 same transgenic line at 10 DAG (bottom panels). YFP signal (green) is counterstained for cell

766 membrane with propidium-iodide (PI, red). Yellow arrows point towards dividing
767 protodermal cells, yellow arrowheads indicate stomatal meristemoids, green arrowheads label
768 fully developed stomata guard cells, blue arrowheads mark elongated pavement cells, and red
769 arrowheads show elongated vascular cells with GFP signal in their nucleus. Scale bars = 20
770 μm (top panels) and 25 μm (bottom panels).

771 (B) Images of wild type (WT) and the transgenic line with high E2FB expression (pgE2FB-
772 GFP line 72) grown for 9 DAG *in vitro* and for 20 DAG on soil. Scale bars = 0.5 cm.

773 (C) Representative images of the abaxial epidermal cell layer of the first leaf pair from WT
774 and pgE2FB-GFP line 72 seedlings (12 DAG) taken by differential interference contrast
775 microscopy (DIC) for which the imprints were made by the gel casting method. An example
776 of elongated puzzle-formed pavement cell is outlined by red colour. Arrows indicate straight
777 cell walls inside the cell, whereas arrowheads mark newly formed cell walls inside the
778 elongated pavement cells. Scale bars = 20 μm .

779 (D) Quantification of the total number of epidermal cells from first leaf pair of the WT and
780 two pgE2FB-GFP transgenic lines (lines 72 and 93). Values represent means and error bars
781 indicate standard deviation (SD). Significance was determined by Student's *t*-test, *a*: *p*-value
782 <0.05. *n*= 3 and *N* > 600. The quantifications of cellular parameters are summarised in
783 Supplemental Table S1 and S2 from 8 DAG and 12 DAG leaves, respectively.

784 Data information *n*= biological repeat, *N*= samples per biological repeat, here and in
785 following Figure legends.

786

787 **Figure 2. RBR efficiently counteracts the excess of E2FB accumulation in proliferating**
788 **but not in differentiating first leaf pairs.**

789

790 (A) Relative expression level of *ORC2*, *CDKB1;1*, *CYCD3;1*, and *RBR* in wild type (WT)
791 and pgE2FB-GFP line 72 from the developing first leaf pair of seedlings 8, 10, 12, and 15
792 days after germination (DAG). Values represent mean of fold change, normalised to the value
793 of the relevant transcript of the WT at 8 DAG, which was set arbitrarily at 1. Error bars: SD.
794 *a*: *p*<0.05, statistical significance determined using Student's *t*-test between WT and the
795 transgenic line at a given time point (*n*=3, *N*>50). Abbreviations of genes and primer
796 sequences are listed in Supplemental Table S3.

797 (B) The phosphorylation level of RBR on the conserved Serine site at 911 position (P-
798 RBR^{S911}) was followed in the developing first leaf pair of two independent pgE2FB-GFP-
799 expressing lines (lines 93 and 72), each with different E2FB protein level, and compared to
800 WT at the indicated time points (DAG) using anti-RBR and P-RBR^{S911}-specific antibody
801 (anti-P-Rb^{807/811}) in immunoblot analysis.

802 (C) To follow RBR accumulation in conjunction to E2FB level, anti-RBR, anti-E2FB, and
803 anti-GFP antibodies were used in immunoblot analysis of proteins in the developing first leaf
804 pair in the same transgenic lines as in (B). In the first panel, the antibody labels RBR (arrow),
805 in the second panel the anti-E2FB antibody labels both the E2FB-GFP (arrow) and the
806 endogenous E2FB (arrowhead), whereas in the third panel the anti-GFP antibody marks the
807 accumulation of the E2FB-GFP fusion protein (arrow).

808 (D) Co-IP of RBR in the E2FB-GFP pull-down was labelled on the immunoblot with anti-
809 RBR. On the same gel, 1/80 of the IP from the extract of the pgE2FB-GFP 72 line was loaded
810 as input. For comparison, in (C) 1/20 of IP was loaded for all genotypes.

811 Non-specific membrane-bound proteins stained by Coomassie-blue were used as loading
812 control (C-D). Note, the quantitation of relative intensities of the protein bands in (B) are
813 shown in Supplemental Figure 4A and 4B, (C) in Supplemental Figure 4C and 4D, whereas
814 the measurement related to proteins in (C and D) are given in Supplemental Figure 4E.

815

816 **Figure 3. E2FB restricts cell proliferation in developing first leaf pair.**

817

818 (A) Total cell number and (B) the ratio of small-sized cells ($<60 \mu\text{m}^2$) in the epidermis of the
819 first leaf pair from wild type (WT), the *e2fb-1* and *e2fb-2* mutant, and from the *e2fb-2* mutant
820 expressing E2FB-GFP under its own promoter (*e2fb-2* E2FB-GFP lines 1 and 2) at 12 days
821 after germination (DAG) (n=3, N>600). Error bars: SD. a: $p<0.05$ statistical significance
822 determined using Student's *t*-test between WT and the two *e2fb* mutants, whereas b: $p<0.05$
823 statistical significance between the complemented lines and *e2fb* mutants.

824 (C) Comparison of the *ORC2*, *MCM3*, *CDKB1;1*, *CYCA2;3*, *CYCD3;1*, and *RBR* transcript
825 levels in the first leaf pair of seedlings of the *e2fb-2* and *e2fb-1* mutants and WT at 8, 10, 12,
826 and 15 DAG. Values represent mean of fold change, normalised to the value of the relevant
827 transcript of the WT at 8 DAG which was arbitrarily set at 1 (n=3, N>50). a: $p<0.05$
828 statistical significance determined using Student's *t*-test between WT and the mutant lines.
829 Error bars: SD. Abbreviations of genes and primer sequences are listed in Supplemental
830 Table S3.

831 (D) Endogenous E2FB and transgenic E2FB-GFP proteins were detected in 1-week-old
832 seedlings from WT and from the two complemented *e2fb-2* E2FB-GFP lines (1 and 2). The
833 arrow indicates the position of E2FB, whereas the arrowhead indicates E2FB-GFP. Non-
834 specific, cross-reacting proteins are used as loading control.

835 **Figure 4. E2FB directly binds to *CYCD3;1*, *CDKB1;1*, and *RBR* promoters.**

836

837 (A) Schematic representation of the *CYCD3;1*, *CDKB1;1*, and *RBR* promoters; arrows
838 labelled p1, p2, or p3 indicate the position of the primer pairs used for qPCR analysis. The

839 position of the canonical E2F elements (white arrowheads) and their distance from the start
840 codon (ATG) are depicted. Primer sequences are listed in Supplemental Table S3.

841 **(B)** Chromatin immunoprecipitation (ChIP) followed by qPCR was carried out on chromatin
842 isolated from complemented *e2fb-2* E2FB-GFP seedlings (7 days after germination; DAG)
843 using polyclonal anti-rabbit GFP antibody; the graph shows fold enrichment calculated as a
844 ratio of chromatin bound to the numbered section of the *CYCD3;1*, *CDKB1;1*, and *RBR*
845 promoters with or without antibody. Shown is a representative experiment of three biological
846 replicates. *a, b*: $p < 0.01$, statistically significant enrichment (*a*) between the relevant fragment
847 and the neighbouring fragments and (*b*) between the relevant regulatory region and the
848 negative control (Actin2) determined by Student's *t*-test. The values represent the means of
849 three technical replicates. Error bars: SD. The enrichment on the Actin2 promoter was
850 arbitrarily set to 1. The labels p1, p2, and p3 on the x-axis refer to the regions indicated in
851 **(A)**.

852

853 **Figure 5. Co-overexpression of *E2FB* and *DPA* results in reduced leaf and cell size.**

854

855 **(A)** Representative images of wild-type (WT) and p35S::HA-E2FB/DPA^{OE} (HA-
856 E2FB/DPA^{OE}) seedlings 8 and 12 days after germination (DAG) grown *in vitro* and 21 DAG
857 grown on soil. Scale bars: 0.5 cm at 8 and 12 DAG; 1 cm at 21 DAG.

858 **(B)** Representative confocal microscopy images of PI-stained abaxial leaf surfaces taken
859 from tip to base of the first leaf pair from WT and HA-E2FB/DPA^{OE} seedlings (8 and 12
860 DAG). Scale bars: 20 μ m.

861 **(C)** Comparison of *E2FB* expression levels in the developing first leaf pair of HA-
862 E2FB/DPA^{OE} and WT seedlings at 8, 10, 12, and 15 DAG, where the expression of *E2FB*
863 was set arbitrarily at 1 at each timepoint. Values represent fold change. Error bars: SD
864 referring to technical repeats. The data is from one biological replicate ($N < 50$), the transcript
865 level correlates well with the HA-E2FB protein accumulation illustrated in **(D)**.

866 **(D)** Detection of protein levels of epitope-tagged (HA-E2FB) and endogenous E2FB, DPA,
867 and CDKB1;1 in the first leaf pair of WT and HA-E2FB/DPA^{OE} seedlings at the indicated
868 time points (DAG) using anti-HA, anti-E2FB, anti-DPA, and anti-CDKB1;1 antibodies. The
869 arrowhead indicates the position of HA-tagged E2FB, whereas arrows indicate endogenous
870 E2FB and CDKB1;1 proteins. The asterisk indicates a non-specific protein cross-reaction
871 with the anti-CDKB1;1 antibody. Non-specific membrane-bound proteins stained by
872 Coomassie-blue were used as loading control.

873

874 **Figure 6. Ectopic E2FB/DPA functions as transcriptional activator on cell cycle genes.**

875

876 (A) The expression levels of *ORC2*, *MCM3*, *CDKB1;1*, *CYCD3;1*, and *RBR* were determined
877 in wild-type (WT) and HA-E2FB/DPA^{OE} seedlings by RT-qPCR. Developing first leaf pair
878 was analysed at each time point as indicated. Values represent mean of fold change
879 normalised to values of the relevant transcript from WT at 8 days after germination (DAG)
880 which was set arbitrarily at 1. Error bars: SD, *a*: *p*<0.05 statistical significance between WT
881 and the transgenic line at a given timepoint, whereas *b*: *p*<0.05 significance between two
882 consecutive timepoints determined using Student's *t*-test (*n*=3, *N*>100). Abbreviations of
883 genes and the list of primers used in this study is listed in Supplemental Table S3.

884 (B) Protein level of RBR, P-RBR^{S911}, HA-E2FB, and endogenous E2FB in the developing
885 first leaf pair of WT and HA-E2FB/DPA^{OE} seedlings at 8, 9, and 12 DAG detected using
886 anti-RBR, anti-P-RBR^{S911} (anti-P-Rb^{807/811}), anti-E2FB, and anti-CDKA;1 antibodies in
887 immunoblot assays. Note, the relative intensities of the RBR and P-RBR^{S911} protein bands are
888 quantified in Supplemental Figure S6F and G.

889 (C and D) Co-immunoprecipitation (co-IP) of HA-E2FB with RBR and DPA proteins in WT
890 and HA-E2FB/DPA^{OE} in seedlings at 7 DAG (C) and in first leaf pair at 8 DAG (D). Co-IP
891 of RBR or HA-E2FB proteins with DPA was determined through immunoblot analysis with
892 anti-RBR or anti-E2FB antibodies. 1/25 of the IP from the extract was loaded as input.
893 Asterisk indicates a non-specific protein cross-reaction with the anti-DPA antibody in the
894 input.

895 In panels B and D, anti-CDKA;1 antibody was used as control. In panel C, non-specific
896 membrane-bound proteins stained by Coomassie-blue were used as loading control.
897 Arrowhead in panel B indicates HA-E2FB and arrows mark the positions of endogenous
898 E2FB, DPA, and CDKA;1 in B, C and D, respectively.

899 **Figure 7. Co-expression of the mutant HA-E2FB^{ARBR} with DPA, which is unable to**
900 **transactivate and bind to RBR, hyper-activates meristematic cell divisions in leaf**
901 **epidermis.**

902

903 (A) Representative images of p35S::HA-E2FB^{ARBR}/DPA (HA-E2FB^{ARBR}/DPA), wild type
904 (WT), and p35S::HA-E2FB/DPA (HA-E2FB/DPA^{OE}) plants grown for 20 days on soil. Scale
905 bar: 1 cm.

906 (B) CM images of PI-stained abaxial leaf surfaces from the first leaf pair of WT and HA-
907 E2FB^{ARBR}/DPA seedlings at 10 days after germination (DAG). White outline shows a typical
908 puzzle formed pavement cell. Arrowheads in both images indicate normally dividing
909 meristemoid cells, whereas white circles illustrate clusters of overproliferated meristemoid
910 cells. Scale bars: 20 μm.

911 (C) Total CDK histone H1 kinase activity purified by p13suc1-Sepharose beads is shown and
912 compared to Histone H1 from the first leaf pair at four different developmental time points
913 (8, 10, 12, and 15 DAG). For comparison, CDKA;1 protein level is also shown in the same

914 leaf samples. Commassie-stained non-specific membrane-bound proteins in the range of 50–
915 60 kDa were used as loading controls.

916 **(D)** Co-IP of RBR and DPB proteins in the GFP-E2FB^{ΔRBR} and GFP-E2FA^{ΔRBR} pull-down
917 was labelled with anti-RBR and anti-DPB antibodies. On the same gel, 1/12th of the IP from
918 the extract of the GFP-E2FB^{ΔRBR} and GFP-E2FA^{ΔRBR} lines were loaded as input. Arrows
919 point towards the specific proteins as indicated. The arrowhead indicates a faster migrating
920 DPB protein. Molecular weight markers are indicated on the left.

921 **(E)** The expression level of *ORC2*, *CDKB1;1*, *CYCD3;1*, and *RBR* was followed in two
922 independent HA-E2FB Δ RBR/DPA lines (lines 10 and 1) using RT-qPCR. The developing
923 first leaf pair was analysed at each time point as indicated. Values represent fold change
924 normalised to values of the relevant transcript from WT at 8 DAG, which was set arbitrarily
925 at 1. As the two independent lines show the same tendencies, here n=2, N>50. *a*: *p*<0.05
926 statistical significance between WT and the transgenic line at a given timepoint determined
927 using Student's *t*-test.

928

929 **Figure 8. Model explaining the functions of E2FB during leaf development.**

930

931 E2FB has three different activities, each is being dominant **(A)** at different leaf
932 developmental stage or **(B)** in different cell types.

933 **(A)** Activator E2FB is in its RBR-free form, characteristic of that in young leaves consisting
934 of mostly proliferating cells. The young meristematic leaf is a nutrient-rich sink-tissue where
935 E2FB is released from the repression of RBR by the CYCD3;1-regulated RBR kinase in a
936 sucrose-dependent manner. E2FB controls the activity of RBR by regulating both its
937 transcriptional and protein level as well as its phosphorylation status by controlling CYCD3;1
938 activity.

939 In leaf cells where the growth-promoting signal is weakened, the protein level of both E2FB
940 and RBR decreases and RBR becomes more active (less phosphorylated) to bind and inhibit
941 E2FB. This repression is important to establish quiescence in leaf cells committed to
942 differentiate.

943 **(B)** In developing leaves, E2FB also forms a repressor complex with RBR in meristemoid
944 leaf cells to co-repress their divisions. How this repression is regulated by up-stream signal(s)
945 is hitherto unknown.

946

947

948 **LITERATURE CITED**

- 949 **Abraham Z, del Pozo JC** (2012) Ectopic Expression of E2FB, a Cell Cycle Transcription
950 Factor, Accelerates Flowering and Increases Fruit Yield in Tomato. *Journal of Plant*
951 *Growth Regulation* **31**: 11-24
- 952 **Andriankaja M, Dhondt S, De Bodt S, Vanhaeren H, Coppens F, De Milde L,**
953 **Muhlenbock P, Skirycz A, Gonzalez N, Beemster GT, Inze D** (2012) Exit from
954 proliferation during leaf development in *Arabidopsis thaliana*: a not-so-gradual
955 process. *Dev Cell* **22**: 64-78
- 956 **Asl LK, Dhondt S, Boudolf V, Beemster GT, Beeckman T, Inze D, Govaerts W, De**
957 **Veylder L** (2011) Model-based analysis of *Arabidopsis* leaf epidermal cells reveals
958 distinct division and expansion patterns for pavement and guard cells. *Plant Physiol*
959 **156**: 2172-2183
- 960 **Berckmans B, Lammens T, Van Den Daele H, Magyar Z, Bogre L, De Veylder L** (2011)
961 Light-dependent regulation of DEL1 is determined by the antagonistic action of E2Fb
962 and E2Fc. *Plant Physiol* **157**: 1440-1451
- 963 **Berckmans B, Vassileva V, Schmid SP, Maes S, Parizot B, Naramoto S, Magyar Z,**
964 **Alvim Kamei CL, Koncz C, Bogre L, Persiau G, De Jaeger G, Friml J, Simon R,**
965 **Beeckman T, De Veylder L** (2011) Auxin-dependent cell cycle reactivation through
966 transcriptional regulation of *Arabidopsis* E2Fa by lateral organ boundary proteins.
967 *Plant Cell* **23**: 3671-3683
- 968 **Bogre L, Magyar Z, Lopez-Juez E** (2008) New clues to organ size control in plants.
969 *Genome Biol* **9**: 226
- 970 **Borghi L, Gutzat R, Futterer J, Laizet Y, Hennig L, Gruissem W** (2010) *Arabidopsis*
971 RETINOBLASTOMA-RELATED is required for stem cell maintenance, cell
972 differentiation, and lateral organ production. *Plant Cell* **22**: 1792-1811
- 973 **Borghi L, Gutzat R, Futterer J, Laizet Y, Hennig L, Gruissem W** (2010) *Arabidopsis*
974 RETINOBLASTOMA-RELATED Is Required for Stem Cell Maintenance, Cell
975 Differentiation, and Lateral Organ Production. *Plant Cell* **22**: 1792-1811
- 976 **Chen HZ, Tsai SY, Leone G** (2009) Emerging roles of E2Fs in cancer: an exit from cell
977 cycle control. *Nat Rev Cancer* **9**: 785-797
- 978 **Clough SJ, Bent AF** (1998) Floral dip: a simplified method for *Agrobacterium*-mediated
979 transformation of *Arabidopsis thaliana*. *Plant J* **16**: 735-743
- 980 **de Jager SM, Scofield S, Huntley RP, Robinson AS, den Boer BG, Murray JA** (2009)
981 Dissecting regulatory pathways of G1/S control in *Arabidopsis*: common and distinct
982 targets of CYCD3;1, E2Fa and E2Fc. *Plant Mol Biol* **71**: 345-365
- 983 **De Veylder L, Beeckman T, Beemster GT, de Almeida Engler J, Ormenese S, Maes S,**
984 **Naudts M, Van Der Schueren E, Jacquard A, Engler G, Inze D** (2002) Control of
985 proliferation, endoreplication and differentiation by the *Arabidopsis* E2Fa-DPa
986 transcription factor. *EMBO J* **21**: 1360-1368
- 987 **De Veylder L, Beeckman T, Inze D** (2007) The ins and outs of the plant cell cycle. *Nat Rev*
988 *Mol Cell Biol* **8**: 655-665
- 989 **De Veylder L, Larkin JC, Schnittger A** (2011) Molecular control and function of
990 endoreplication in development and physiology. *Trends Plant Sci* **16**: 624-634
- 991 **del Pozo JC, Diaz-Trivino S, Cisneros N, Gutierrez C** (2006) The balance between cell
992 division and endoreplication depends on E2FC-DPB, transcription factors regulated
993 by the ubiquitin-SCFSKP2A pathway in *Arabidopsis*. *Plant Cell* **18**: 2224-2235
- 994 **Dong J, MacAlister CA, Bergmann DC** (2009) BASL controls asymmetric cell division in
995 *Arabidopsis*. *Cell* **137**: 1320-1330
- 996 **Doonan J, Hunt T** (1996) Cell cycle. Why don't plants get cancer? *Nature* **380**: 481-482

- 997 **Galinha C, Hofhuis H, Luijten M, Willemsen V, Blilou I, Heidstra R, Scheres B** (2007)
 998 PLETHORA proteins as dose-dependent master regulators of Arabidopsis root
 999 development. *Nature* **449**: 1053-1057
- 1000 **Gazquez A, Beemster GTS** (2017) What determines organ size differences between species?
 1001 A meta-analysis of the cellular basis. *New Phytol* **215**: 299-308
- 1002 **Harashima H, Sugimoto K** (2016) Integration of developmental and environmental signals
 1003 into cell proliferation and differentiation through RETINOBLASTOMA-RELATED
 1004 1. *Curr Opin Plant Biol* **29**: 95-103
- 1005 **Henriques R, Magyar Z, Bogre L** (2013) S6K1 and E2FB are in mutually antagonistic
 1006 regulatory links controlling cell growth and proliferation in Arabidopsis. *Plant Signal*
 1007 *Behav* **8**: e24367
- 1008 **Henriques R, Magyar Z, Monardes A, Khan S, Zalejski C, Orellana J, Szabados L, de**
 1009 **la Torre C, Koncz C, Bogre L** (2010) Arabidopsis S6 kinase mutants display
 1010 chromosome instability and altered RBR1-E2F pathway activity. *EMBO J* **29**: 2979-
 1011 2993
- 1012 **Heyman J, Van den Daele H, De Wit K, Boudolf V, Berckmans B, Verkest A, Alvim**
 1013 **Kamei CL, De Jaeger G, Koncz C, De Veylder L** (2011) Arabidopsis
 1014 ULTRAVIOLET-B-INSENSITIVE4 maintains cell division activity by temporal
 1015 inhibition of the anaphase-promoting complex/cyclosome. *Plant Cell* **23**: 4394-4410
- 1016 **Horiguchi G, Fujikura U, Ferjani A, Ishikawa N, Tsukaya H** (2006) Large-scale
 1017 histological analysis of leaf mutants using two simple leaf observation methods:
 1018 identification of novel genetic pathways governing the size and shape of leaves. *Plant*
 1019 *J* **48**: 638-644
- 1020 **Horvath BM, Kourova H, Nagy S, Nemeth E, Magyar Z, Papdi C, Ahmad Z, Sanchez-**
 1021 **Perez GF, Perilli S, Blilou I, Pettko-Szandtner A, Darula Z, Meszaros T,**
 1022 **Binarova P, Bogre L, Scheres B** (2017) Arabidopsis RETINOBLASTOMA
 1023 RELATED directly regulates DNA damage responses through functions beyond cell
 1024 cycle control. *EMBO J* **36**: 1261-1278
- 1025 **Johnson DG, Schwarz JK, Cress WD, Nevins JR** (1993) Expression of transcription factor
 1026 E2F1 induces quiescent cells to enter S phase. *Nature* **365**: 349-352
- 1027 **Kalve S, De Vos D, Beemster GT** (2014) Leaf development: a cellular perspective. *Front*
 1028 *Plant Sci* **5**: 362
- 1029 **Karimi M, Inze D, Depicker A** (2002) GATEWAY vectors for Agrobacterium-mediated
 1030 plant transformation. *Trends Plant Sci* **7**: 193-195
- 1031 **Kobayashi K, Suzuki T, Iwata E, Magyar Z, Bogre L, Ito M** (2015) MYB3Rs, plant
 1032 homologs of Myb oncoproteins, control cell cycle-regulated transcription and form
 1033 DREAM-like complexes. *Transcription* **6**: 106-111
- 1034 **Kobayashi K, Suzuki T, Iwata E, Nakamichi N, Chen P, Ohtani M, Ishida T, Hosoya H,**
 1035 **Muller S, Leviczky T, Pettko-Szandtner A, Darula Z, Iwamoto A, Nomoto M,**
 1036 **Tada Y, Higashiyama T, Demura T, Doonan JH, Hauser MT, Sugimoto K,**
 1037 **Umeda M, Magyar Z, Bogre L, Ito M** (2015) Transcriptional repression by MYB3R
 1038 proteins regulates plant organ growth. *EMBO J* **34**: 1992-2007
- 1039 **Kosugi S, Ohashi Y** (2002) Interaction of the Arabidopsis E2F and DP proteins confers their
 1040 concomitant nuclear translocation and transactivation. *Plant Physiology* **128**: 833-843
- 1041 **Li X, Cai W, Liu Y, Li H, Fu L, Liu Z, Xu L, Liu H, Xu T, Xiong Y** (2017) Differential
 1042 TOR activation and cell proliferation in Arabidopsis root and shoot apices. *Proc Natl*
 1043 *Acad Sci U S A* **114**: 2765-2770
- 1044 **Magyar Z, Atanassova A, De Veylder L, Rombauts S, Inze D** (2000) Characterization of
 1045 two distinct DP-related genes from Arabidopsis thaliana. *FEBS Lett* **486**: 79-87

- 1046 **Magyar Z, Bogre L, Ito M** (2016) DREAMs make plant cells to cycle or to become
 1047 quiescent. *Curr Opin Plant Biol* **34**: 100-106
- 1048 **Magyar Z, De Veylder L, Atanassova A, Bako L, Inze D, Bogre L** (2005) The role of the
 1049 Arabidopsis E2FB transcription factor in regulating auxin-dependent cell division.
 1050 *Plant Cell* **17**: 2527-2541
- 1051 **Magyar Z, Horvath B, Khan S, Mohammed B, Henriques R, De Veylder L, Bako L,**
 1052 **Scheres B, Bogre L** (2012) Arabidopsis E2FA stimulates proliferation and endocycle
 1053 separately through RBR-bound and RBR-free complexes. *EMBO J* **31**: 1480-1493
- 1054 **Magyar Z, Meszaros T, Miskolczi P, Deak M, Feher A, Brown S, Kondorosi E,**
 1055 **Athanasiadis A, Pongor S, Bilgin M, Bako L, Koncz C, Dudits D** (1997) Cell cycle
 1056 phase specificity of putative cyclin-dependent kinase variants in synchronized alfalfa
 1057 cells. *Plant Cell* **9**: 223-235
- 1058 **Mariconti L, Pellegrini B, Cantoni R, Stevens R, Bergounioux C, Cella R, Albani D**
 1059 (2002) The E2F family of transcription factors from Arabidopsis thaliana. Novel and
 1060 conserved components of the retinoblastoma/E2F pathway in plants. *J Biol Chem*
 1061 **277**: 9911-9919
- 1062 **Matos JL, Lau OS, Hachez C, Cruz-Ramirez A, Scheres B, Bergmann DC** (2014)
 1063 Irreversible fate commitment in the Arabidopsis stomatal lineage requires a FAMA
 1064 and RETINOBLASTOMA-RELATED module. *Elife* **3**
- 1065 **Morgan DO** (2007) *The Cell Cycle: Principles of Control*. Oxford University Press
- 1066 **Sadasivam S, DeCaprio JA** (2013) The DREAM complex: master coordinator of cell cycle-
 1067 dependent gene expression. *Nat Rev Cancer* **13**: 585-595
- 1068 **Saleh A, Alvarez-Venegas R, Avramova Z** (2008) An efficient chromatin
 1069 immunoprecipitation (ChIP) protocol for studying histone modifications in
 1070 Arabidopsis plants. *Nat Protoc* **3**: 1018-1025
- 1071 **Simmons AR, Davies KA, Wang W, Liu Z, Bergmann DC** (2019) SOL1 and SOL2
 1072 regulate fate transition and cell divisions in the Arabidopsis stomatal lineage.
 1073 *Development*
- 1074 **Sozzani R, Maggio C, Varotto S, Canova S, Bergounioux C, Albani D, Cella R** (2006)
 1075 Interplay between Arabidopsis activating factors E2Fb and E2Fa in cell cycle
 1076 progression and development. *Plant Physiology* **140**: 1355-1366
- 1077 **Umbrasaitė J, Schweighofer A, Kazanaviciute V, Magyar Z, Ayatollahi Z,**
 1078 **Unterwurzacher V, Choopayak C, Boniecka J, Murray JA, Bogre L, Meskiene I**
 1079 (2010) MAPK phosphatase AP2C3 induces ectopic proliferation of epidermal cells
 1080 leading to stomata development in Arabidopsis. *PLoS One* **5**: e15357
- 1081 **van den Heuvel S, Dyson NJ** (2008) Conserved functions of the pRB and E2F families. *Nat*
 1082 *Rev Mol Cell Biol* **9**: 713-724
- 1083 **White DW** (2006) PEAPOD regulates lamina size and curvature in Arabidopsis. *Proc Natl*
 1084 *Acad Sci U S A* **103**: 13238-13243
- 1085 **Xie Z, Lee E, Lucas JR, Morohashi K, Li D, Murray JA, Sack FD, Grotewold E** (2010)
 1086 Regulation of cell proliferation in the stomatal lineage by the Arabidopsis MYB
 1087 FOUR LIPS via direct targeting of core cell cycle genes. *Plant Cell* **22**: 2306-2321
- 1088 **Yang K, Wang H, Xue S, Qu X, Zou J, Le J** (2014) Requirement for A-type cyclin-
 1089 dependent kinase and cyclins for the terminal division in the stomatal lineage of
 1090 Arabidopsis. *J Exp Bot* **65**: 2449-2461
- 1091 **Zacksenhaus E, Jiang Z, Chung D, Marth JD, Phillips RA, Gallie BL** (1996) pRb
 1092 controls proliferation, differentiation, and death of skeletal muscle cells and other
 1093 lineages during embryogenesis. *Genes Dev* **10**: 3051-3064

1094 **Zhang X, Henriques R, Lin SS, Niu QW, Chua NH** (2006) Agrobacterium-mediated
1095 transformation of *Arabidopsis thaliana* using the floral dip method. *Nat Protoc* **1**: 641-
1096 646

Figure 1

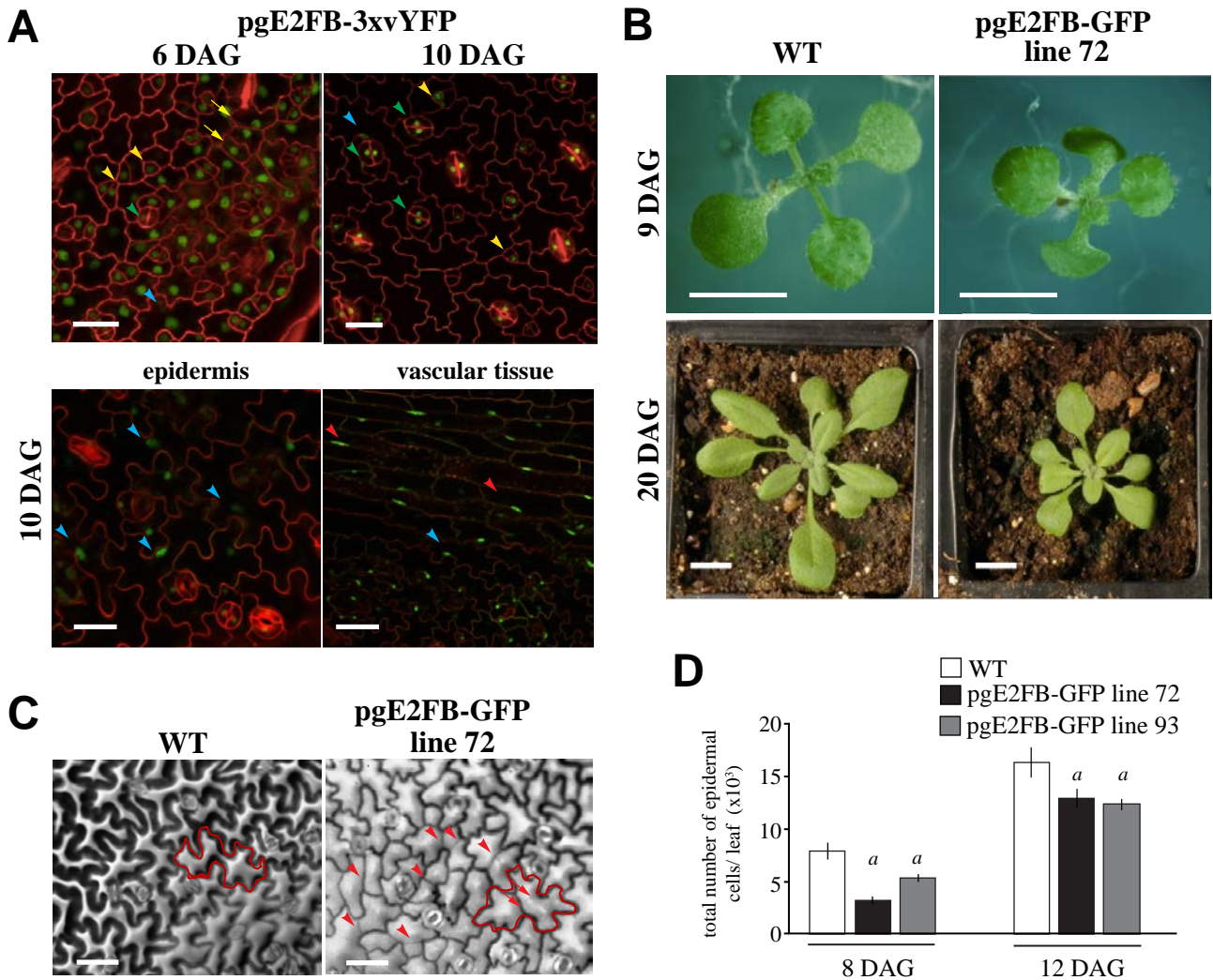


Figure 1. Elevated E2FB level in its own expression domain inhibits cell proliferation in young leaves and disturbs quiescence in older leaves.

(A) Representative confocal laser scanning microscopy (CM) images of the abaxial leaf surface from the first leaf pair of the transgenic line pgE2FB-3xvYFP at 6 and 10 days after germination (DAG; top panels), and localisation in the epidermis and vascular tissues of the same transgenic line at 10 DAG (bottom panels). YFP signal (green) is counterstained for cell membrane with propidium-iodide (PI, red). Yellow arrows point towards dividing protodermal cells, yellow arrowheads indicate stomatal meristemoids, green arrowheads label fully developed stomata guard cells, blue arrowheads mark elongated pavement cells, and red arrowheads show elongated vascular cells with GFP signal in their nucleus. Scale bars = 20 μ m (top panels) and 25 μ m (bottom panels).

(B) Images of wild type (WT) and the transgenic line with high E2FB expression (pgE2FB-GFP line 72) grown for 9 DAG *in vitro* and for 20 DAG on soil. Scale bars = 0.5 cm.

(C) Representative images of the abaxial epidermal cell layer of the first leaf pair from WT and pgE2FB-GFP line 72 seedlings (12 DAG) taken by differential interference contrast microscopy (DIC) for which the imprints were made by the gel casting method. An example of elongated puzzle-formed pavement cell is outlined by red colour. Arrows indicate straight cell walls inside the cell, whereas arrowheads mark newly formed cell walls inside the elongated pavement cells. Scale bars = 20 μ m.

(D) Quantification of the total number of epidermal cells from first leaf pair of the WT and two pgE2FB-GFP transgenic lines (lines 72 and 93). Values represent means and error bars indicate standard deviation (SD). Significance was determined by Student's *t*-test, *a*: *p*-value < 0.05. *n* = 3 and *N* > 600. The quantifications of cellular parameters are summarised in Supplemental Table S1 and S2 from 8 DAG and 12 DAG leaves, respectively.

Data information *n* = biological repeat, *N* = samples per biological repeat, here and in following Figure legends.

Figure 2

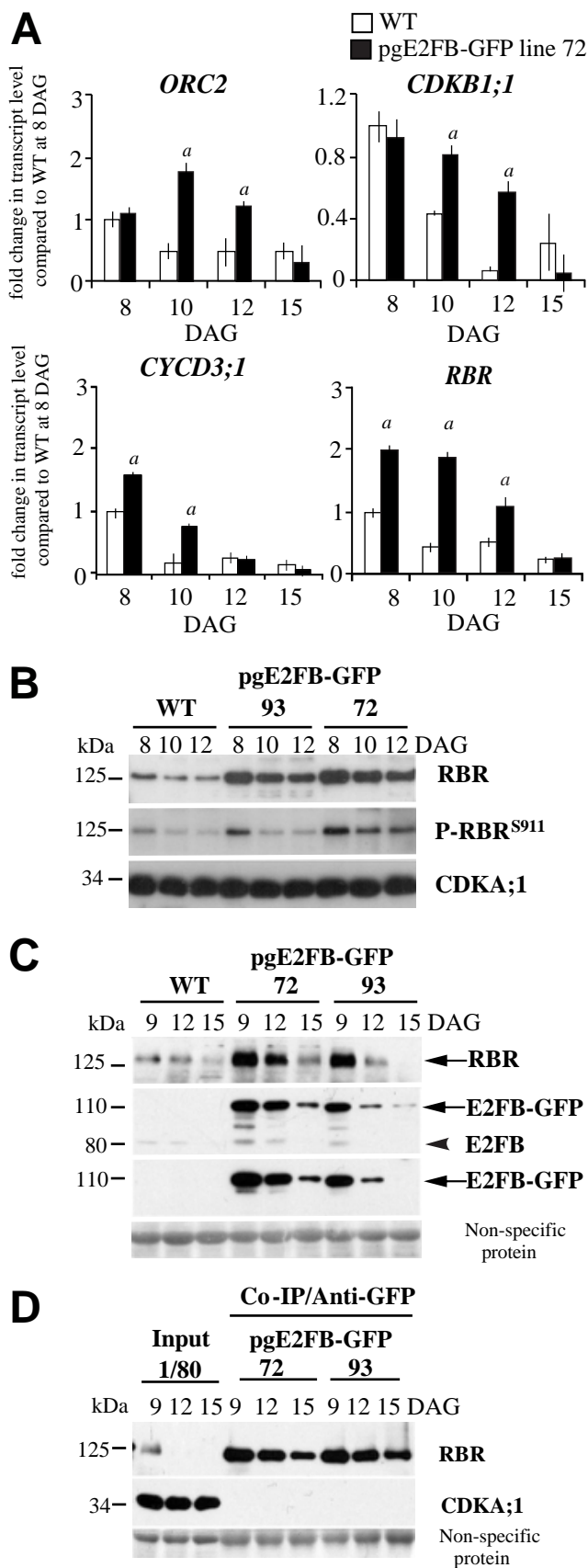


Figure 2. RBR efficiently counteracts excess of E2FB accumulation in proliferating but not in differentiating first leaf pairs.

(A) Relative expression level of *ORC2*, *CDKB1;1*, *CYCD3;1*, and *RBR* in wild type (WT) and pgE2FB-GFP line 72 from the developing first leaf pair of seedlings 8, 10, 12, and 15 days after germination (DAG). Values represent mean of fold change, normalised to the value of the relevant transcript of the WT at 8 DAG, which was set arbitrarily at 1. Error bars: SD. *a*: $p < 0.05$, statistical significance determined using Student's *t*-test between WT and the transgenic line at a given time point ($n=3$, $N > 50$). Abbreviations of genes and primer sequences are listed in Supplemental Table S3.

(B) The phosphorylation level of RBR on the conserved Serine site at 911 position (P-RBR^{S911}) was followed in the developing first leaf pair of two independent pgE2FB-GFP-expressing lines (lines 93 and 72), each with different E2FB protein level, and compared to WT at the indicated time points (DAG) using anti-RBR and P-RBR^{S911}-specific antibody (anti-P-Rb^{807/811}) in immunoblot analysis.

(C) To follow RBR accumulation in conjunction to E2FB level, anti-RBR, anti-E2FB, and anti-GFP antibodies were used in immunoblot analysis of proteins in the developing first leaf pair in the same transgenic lines as in (B). In the first panel, the antibody labels RBR (arrow), in the second panel the anti-E2FB antibody labels both the E2FB-GFP (arrow) and the endogenous E2FB (arrowhead), whereas in the third panel the anti-GFP antibody marks the accumulation of the E2FB-GFP fusion protein (arrow).

(D) Co-IP of RBR in the E2FB-GFP pull-down was labelled on the immunoblot with anti-RBR. On the same gel, 1/80 of the IP from the extract of the pgE2FB-GFP 72 line was loaded as input. For comparison, in (C) 1/20 of IP was loaded for all genotypes.

Non-specific membrane-bound proteins stained by Coomassie-blue were used as loading control (C-D). Note, the quantitation of relative intensities of the protein bands in (B) are shown in Supplemental Figure 4A and 4B, (C) in Supplemental Figure 4C and 4D, whereas the measurement related to proteins in (C and D) are given in Supplemental Figure 4E.

Figure 3

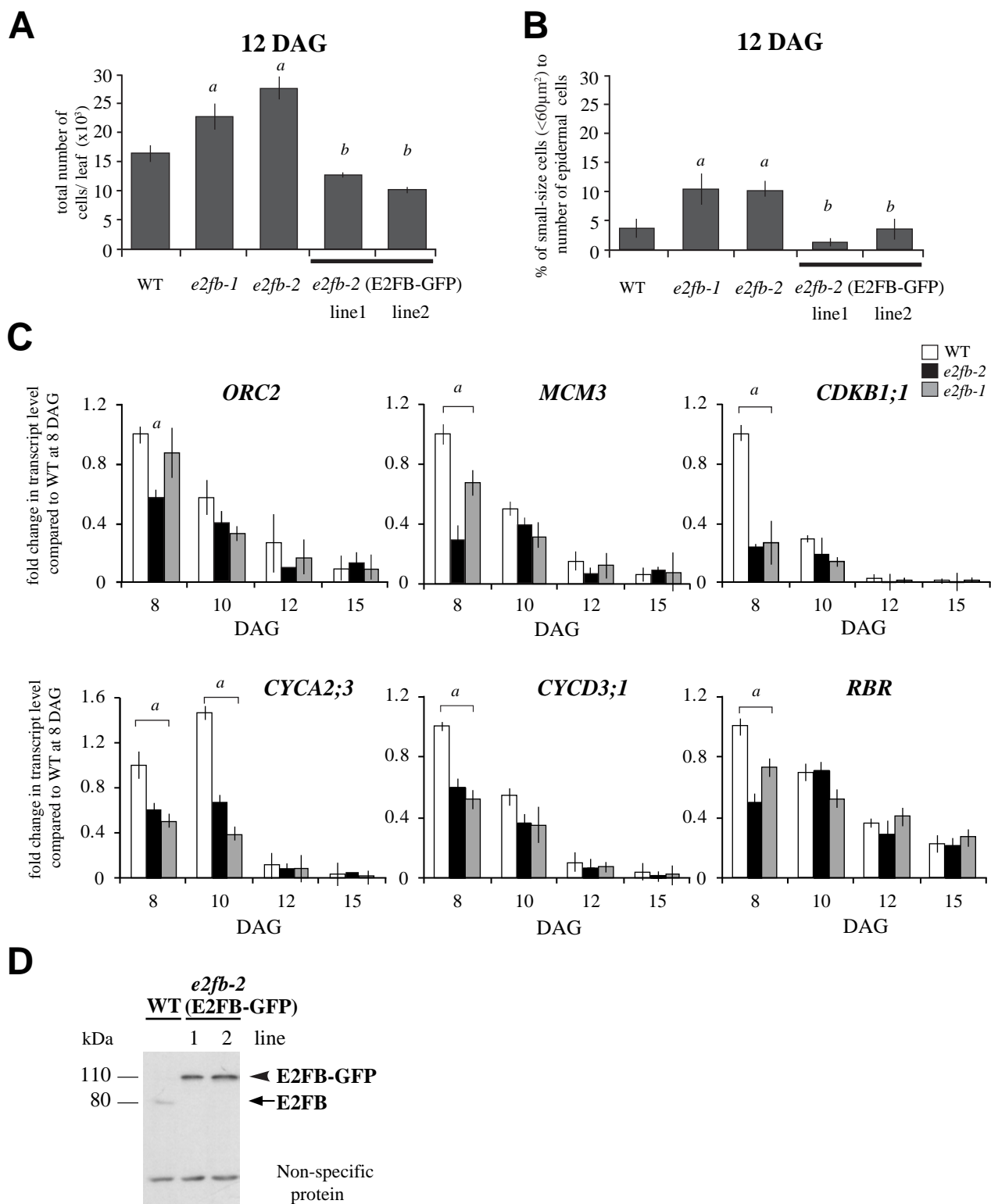


Figure 3. E2FB restricts cell proliferation in developing first leaf pair.

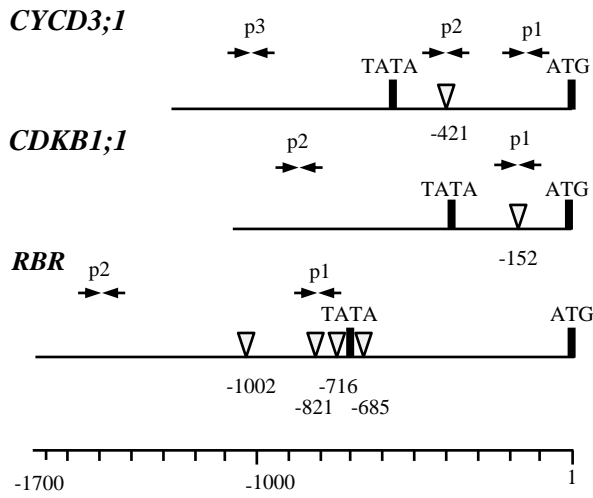
(A) Total cell number and (B) the ratio of small-sized cells (<60 μm^2) in the epidermis of the first leaf pair from wild type (WT), the *e2fb-1* and *e2fb-2* mutant, and from the *e2fb-2* mutant expressing E2FB-GFP under its own promoter (*e2fb-2* E2FB-GFP lines 1 and 2) at 12 days after germination (DAG) (n=3, N>600). Error bars: SD. *a*: $p < 0.05$ statistical significance determined using Student's *t*-test between WT and the two *e2fb* mutants, whereas *b*: $p < 0.05$ statistical significance between the complemented lines and *e2fb* mutants.

(C) Comparison of the *ORC2*, *MCM3*, *CDKB1;1*, *CYCA2;3*, *CYCD3;1*, and *RBR* transcript levels in the first leaf pair of seedlings of the *e2fb-2* and *e2fb-1* mutants and WT at 8, 10, 12, and 15 DAG. Values represent mean of fold change, normalised to the value of the relevant transcript of the WT at 8 DAG which was arbitrarily set at 1 (n=3, N>50). *a*: $p < 0.05$ statistical significance determined using Student's *t*-test between WT and the mutant lines. Error bars: SD. Abbreviations of genes and primer sequences are listed in Supplemental Table S3.

(D) Endogenous E2FB and transgenic E2FB-GFP proteins were detected in 1-week-old seedlings from WT and from the two complemented *e2fb-2* E2FB-GFP lines (1 and 2). The arrow indicates the position of E2FB, whereas the arrowhead indicates E2FB-GFP. Non-specific, cross-reacting proteins are used as loading control.

Figure 4

A



B

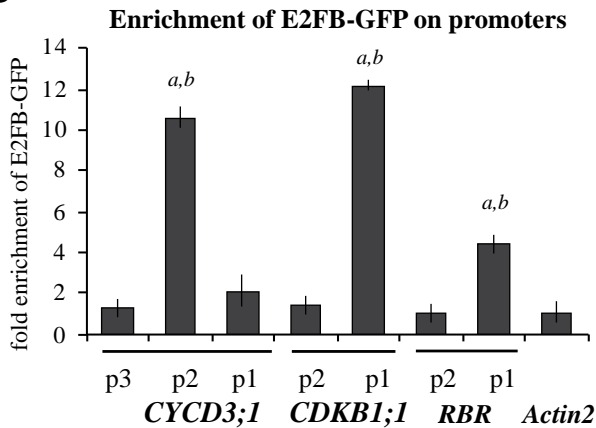


Figure 4. E2FB directly binds to *CYCD3;1*, *CDKB1;1*, and *RBR* promoters.

(A) Schematic representation of the *CYCD3;1*, *CDKB1;1*, and *RBR* promoters; arrows labelled p1, p2, or p3 indicate the position of the primer pairs used for qPCR analysis. The position of the canonical E2F elements (white arrowheads) and their distance from the start codon (ATG) are depicted. Primer sequences are listed in Supplemental Table S3.

(B) Chromatin immunoprecipitation (ChIP) followed by qPCR was carried out on chromatin isolated from complemented *e2fb-2* E2FB-GFP seedlings (7 days after germination; DAG) using polyclonal anti-rabbit GFP antibody; the graph shows fold enrichment calculated as a ratio of chromatin bound to the numbered section of the *CYCD3;1*, *CDKB1;1*, and *RBR* promoters with or without antibody. Shown is a representative experiment of three biological replicates. *a, b*: $p < 0.01$, statistically significant enrichment (*a*) between the relevant fragment and the neighbouring fragments and (*b*) between the relevant regulatory region and the negative control (Actin2) determined by Student's *t*-test. The values represent the means of three technical replicates. Error bars: SD. The enrichment on the Actin2 promoter was arbitrarily set to 1. The labels p1, p2, and p3 on the x-axis refer to the regions indicated in (A).

Figure 5

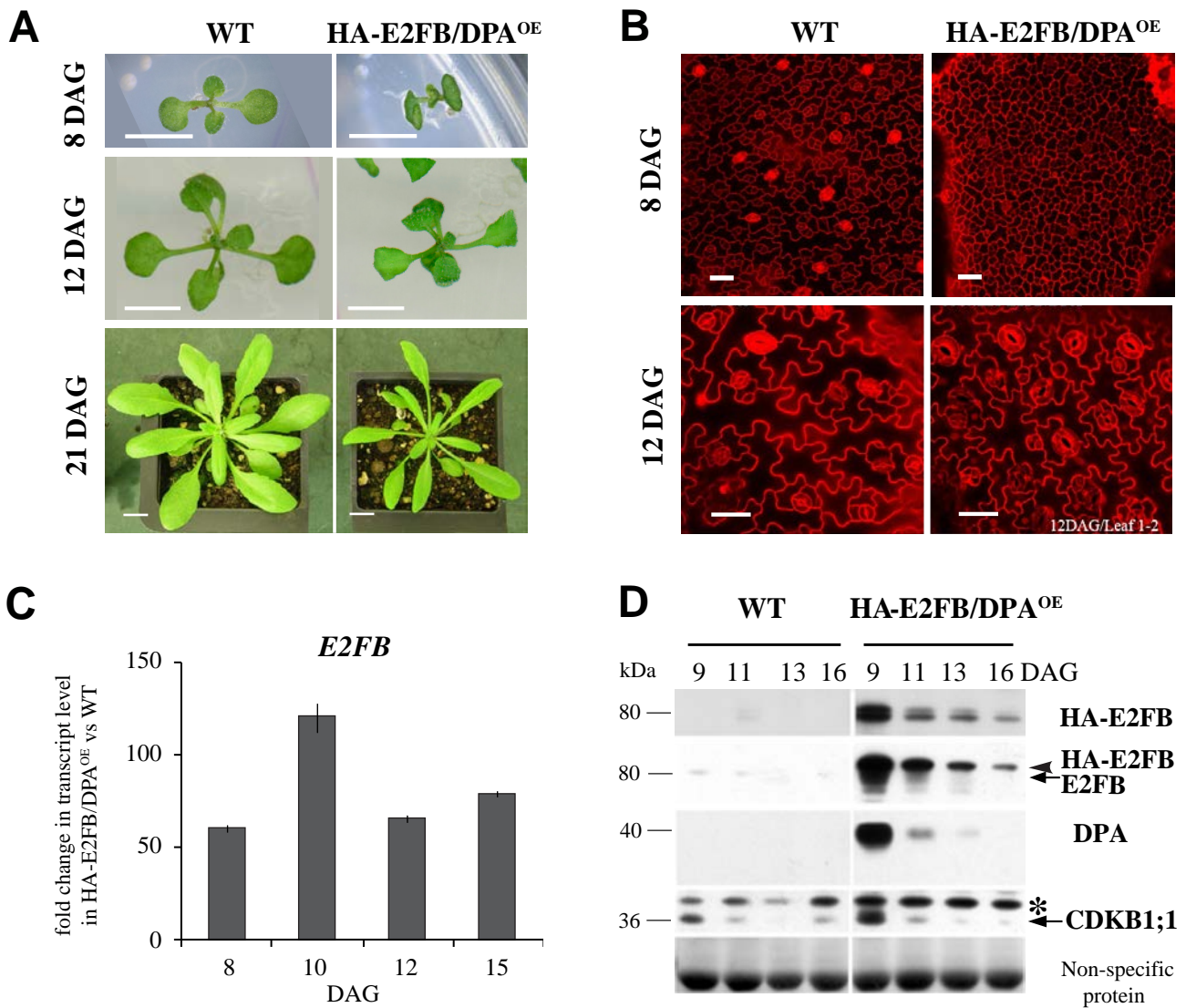


Figure 5. Co-overexpression of *E2FB* and *DPA* results in reduced leaf and cell size.

(A) Representative images of wild-type (WT) and p35S::HA-E2FB/*DPA*^{OE} (HA-E2FB/*DPA*^{OE}) seedlings 8 and 12 days after germination (DAG) grown *in vitro* and 21 DAG grown on soil. Scale bars: 0.5 cm at 8 and 12 DAG; 1 cm at 21 DAG.

(B) Representative confocal microscopy images of PI-stained abaxial leaf surfaces taken from tip to base of the first leaf pair from WT and HA-E2FB/*DPA*^{OE} seedlings (8 and 12 DAG). Scale bars: 20 μ m.

(C) Comparison of *E2FB* expression levels in the developing first leaf pair of HA-E2FB/*DPA*^{OE} and WT seedlings at 8, 10, 12, and 15 DAG, where the expression of *E2FB* was set arbitrarily at 1 at each timepoint. Values represent fold change. Error bars: SD referring to technical repeats. The data is from one biological replicate (N<50), the transcript level correlates well with the HA-E2FB protein accumulation illustrated in (D).

(D) Detection of protein levels of epitope-tagged (HA-E2FB) and endogenous E2FB, *DPA*, and CDKB1;1 in the first leaf pair of WT and HA-E2FB/*DPA*^{OE} seedlings at the indicated time points (DAG) using anti-HA, anti-E2FB, anti-*DPA*, and anti-CDKB1;1 antibodies. The arrowhead indicates the position of HA-tagged E2FB, whereas arrows indicate endogenous E2FB and CDKB1;1 proteins. The asterisk indicates a non-specific protein cross-reaction with the anti-CDKB1;1 antibody. Non-specific membrane-bound proteins stained by Coomassie-blue were used as loading control.

Figure 6

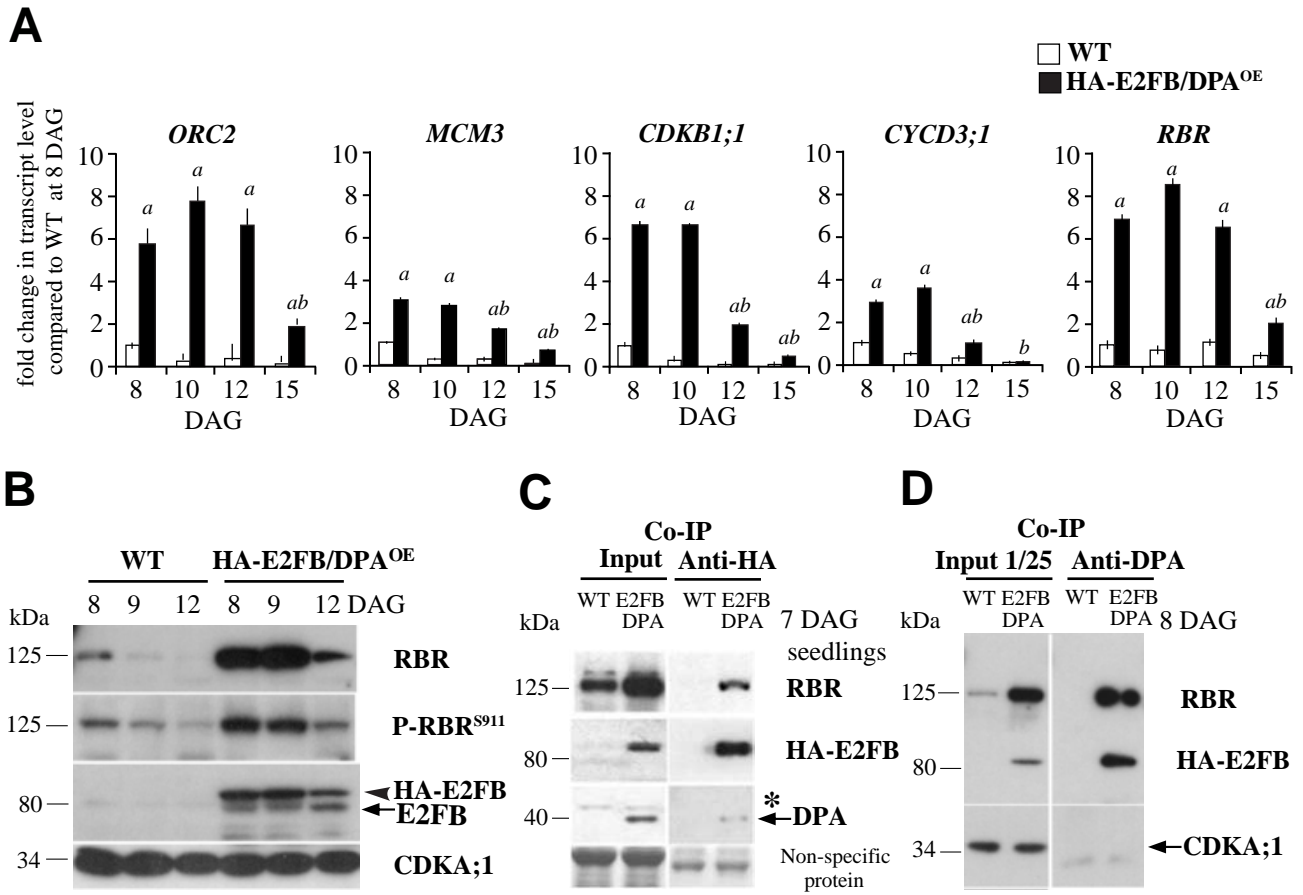


Figure 6. Ectopic E2FB/DPA functions as transcriptional activator on cell cycle genes.

(A) The expression levels of *ORC2*, *MCM3*, *CDKB1;1*, *CYCD3;1*, and *RBR* were determined in wild-type (WT) and HA-E2FB/DPA^{OE} seedlings by RT-qPCR. Developing first leaf pair was analysed at each time point as indicated. Values represent mean of fold change normalised to values of the relevant transcript from WT at 8 days after germination (DAG) which was set arbitrarily at 1. Error bars: SD, *a*: $p < 0.05$ statistical significance between WT and the transgenic line at a given timepoint, whereas *b*: $p < 0.05$ significance between two consecutive timepoints determined using Student's *t*-test ($n=3$, $N > 100$). Abbreviations of genes and the list of primers used in this study is listed in Supplemental Table S3.

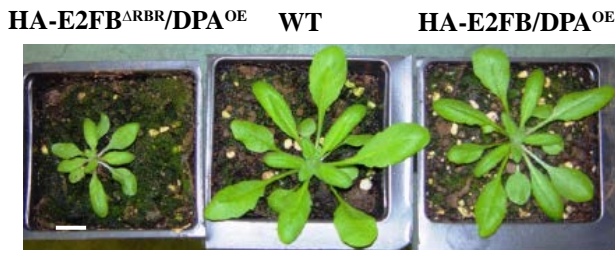
(B) Protein level of RBR, P-RBR^{S911}, HA-E2FB, and endogenous E2FB in the developing first leaf pair of WT and HA-E2FB/DPA^{OE} seedlings at 8, 9, and 12 DAG detected using anti-RBR, anti-P-RBR^{S911} (anti-P-Rb^{807/811}), anti-E2FB, and anti-CDKA;1 antibodies in immunoblot assays. Note, the relative intensities of the RBR and P-RBR^{S911} protein bands are quantified in Supplemental Figure S6F and G.

(C and D) Co-immunoprecipitation (co-IP) of HA-E2FB with RBR and DPA proteins in WT and HA-E2FB/DPA^{OE} in seedlings at 7 DAG (C) and in first leaf pair at 8 DAG (D). Co-IP of RBR or HA-E2FB proteins with DPA was determined through immunoblot analysis with anti-RBR or anti-E2FB antibodies. 1/25 of the IP from the extract was loaded as input. Asterisk indicates a non-specific protein cross-reaction with the anti-DPA antibody in the input.

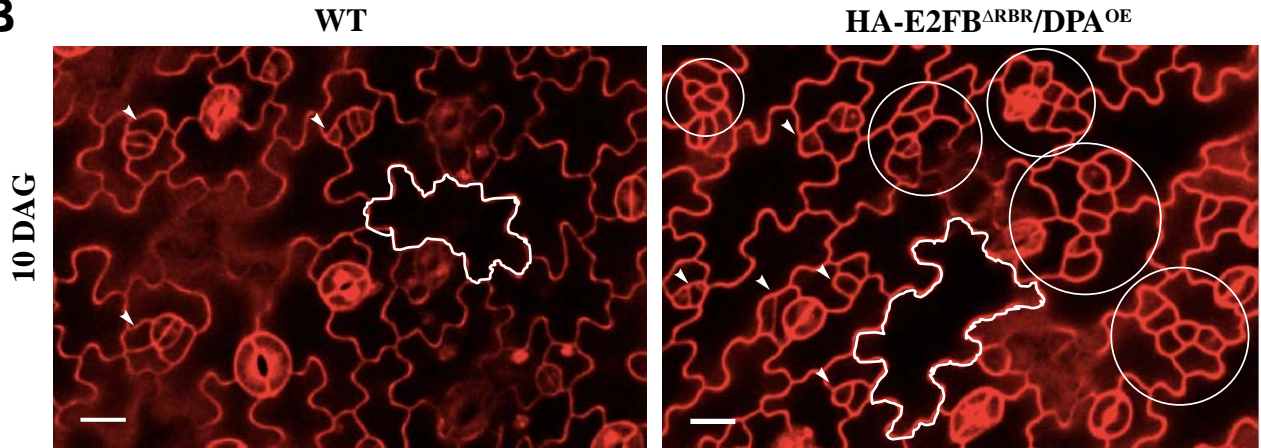
In panels B and D, anti-CDKA;1 antibody was used as control. In panel C, non-specific membrane-bound proteins stained by Coomassie-blue were used as loading control. Arrowhead in panel B indicates HA-E2FB and arrows mark the positions of endogenous E2FB, DPA, and CDKA;1 in B, C and D, respectively

Figure 7

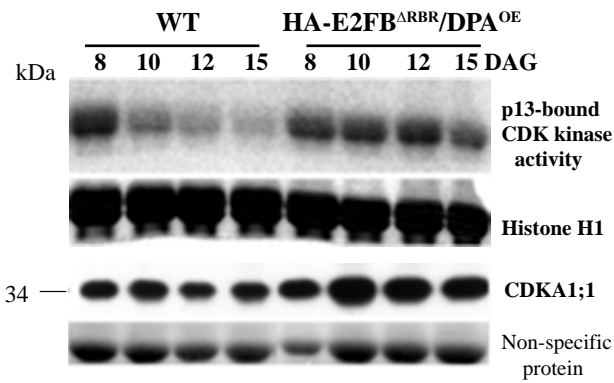
A



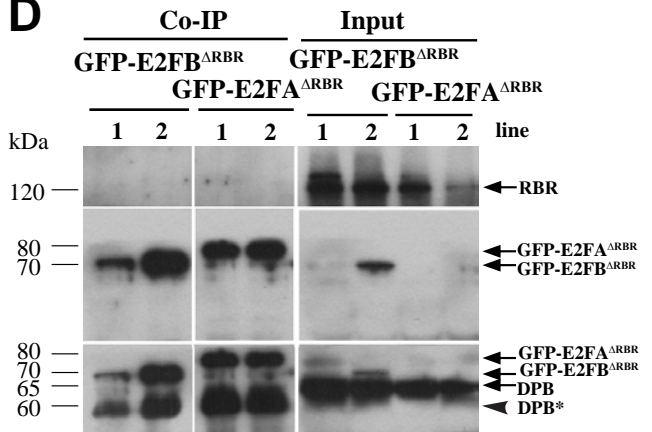
B



C



D



E

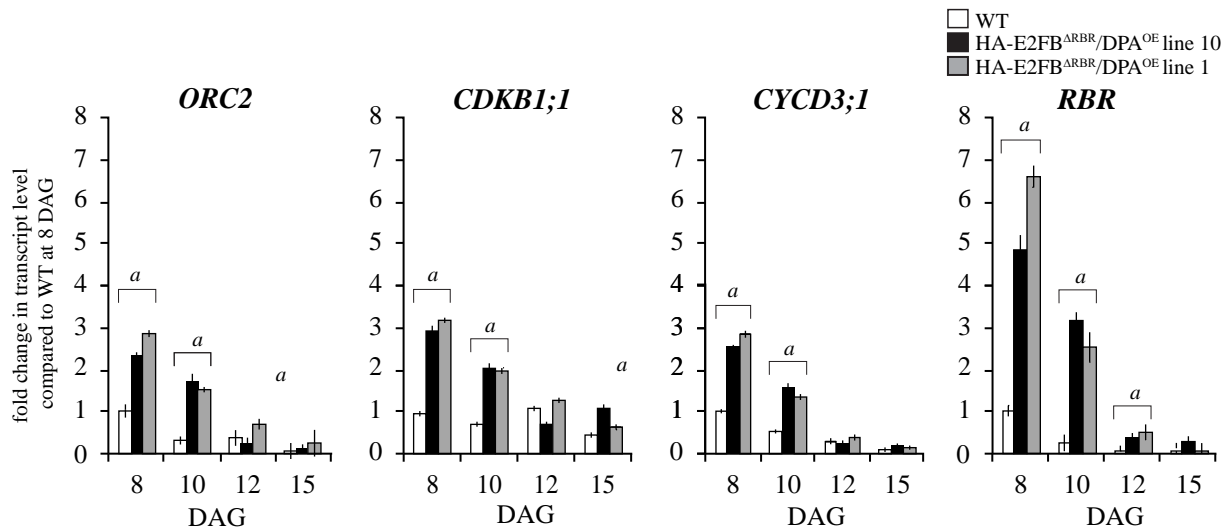


Figure 7. Co-expression of the mutant HA-E2FB^{ARBR} with DPA, which is unable to transactivate and bind to RBR, hyper-activates meristematic cell divisions in leaf epidermis.

(A) Representative images of p35S::HA-E2FB^{ARBR}/DPA (HA-E2FB^{ARBR}/DPA), wild type (WT), and p35S::HA-E2FB/DPA (HA-E2FB/DPA^{OE}) plants grown for 20 days on soil. Scale bar: 1 cm.

(B) CM images of PI-stained abaxial leaf surfaces from the first leaf pair of WT and HA-E2FB^{ARBR}/DPA seedlings at 10 days after germination (DAG). White outline shows a typical puzzle formed pavement cell. Arrowheads in both images indicate normally dividing meristemoid cells, whereas white circles illustrate clusters of overproliferated meristemoid cells. Scale bars: 20 μ m.

(C) Total CDK histone H1 kinase activity purified by p13suc1-Sepharose beads is shown and compared to Histone H1 from the first leaf pair at four different developmental time points (8, 10, 12, and 15 DAG). For comparison, CDKA;1 protein level is also shown in the same leaf samples. Commassie-stained non-specific membrane-bound proteins in the range of 50–60 kDa were used as loading controls.

(D) Co-IP of RBR and DPB proteins in the GFP-E2FB^{ARBR} and GFP-E2FA^{ARBR} pull-down was labelled with anti-RBR and anti-DPB antibodies. On the same gel, 1/12th of the IP from the extract of the GFP-E2FB^{ARBR} and GFP-E2FA^{ARBR} lines were loaded as input. Arrows point towards the specific proteins as indicated. The arrowhead indicates a faster migrating DPB protein. Molecular weight markers are indicated on the left.

(E) The expression level of *ORC2*, *CDKB1;1*, *CYCD3;1*, and *RBR* was followed in two independent HA-E2FB Δ RBR/DPA lines (lines 10 and 1) using RT-qPCR. The developing first leaf pair was analysed at each time point as indicated. Values represent fold change normalised to values of the relevant transcript from WT at 8 DAG, which was set arbitrarily at 1. As the two independent lines show the same tendencies, here n=2, N>50. *a*: *p*<0.05 statistical significance between WT and the transgenic line at a given timepoint determined using Student's *t*-test.

Figure 8

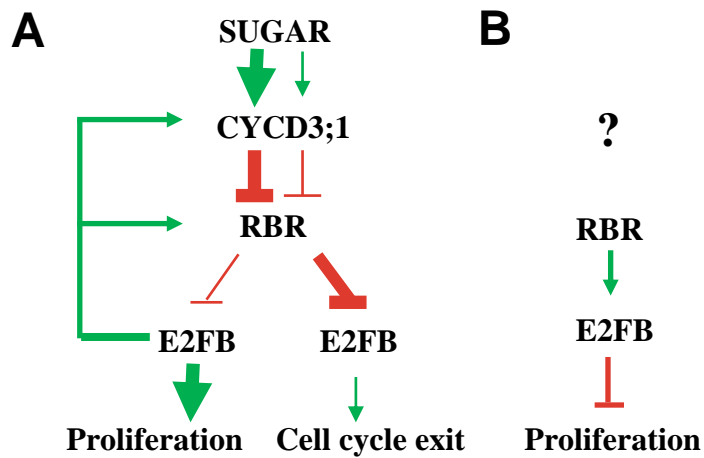


Figure 8. Model explaining the functions of E2FB during leaf development.

E2FB has three different activities, each is being dominant (**A**) at different leaf developmental stage or (**B**) in different cell types.

(**A**) Activator E2FB is in its RBR-free form, characteristic of that in young leaves consisting of mostly proliferating cells. The young meristematic leaf is a nutrient-rich sink-tissue where E2FB is released from the repression of RBR by the CYCD3;1-regulated RBR kinase in a sucrose-dependent manner. E2FB controls the activity of RBR by regulating both its transcriptional and protein level as well as its phosphorylation status by controlling CYCD3;1 activity.

In leaf cells where the growth-promoting signal is weakened, the protein level of both E2FB and RBR decreases and RBR becomes more active (less phosphorylated) to bind and inhibit E2FB. This repression is important to establish quiescence in leaf cells committed to differentiate.

(**B**) In developing leaves, E2FB also forms a repressor complex with RBR in meristemoid leaf cells to co-repress their divisions. How this repression is regulated by up-stream signal(s) is hitherto unknown.

Parsed Citations

Abraham Z, del Pozo JC (2012) Ectopic Expression of E2FB, a Cell Cycle Transcription Factor, Accelerates Flowering and Increases Fruit Yield in Tomato. Journal of Plant Growth Regulation 31: 11-24

Pubmed: [Author and Title](#)

Google Scholar: [Author Only Title Only Author and Title](#)

Andriankaja M, Dhondt S, De Bodt S, Vanhaeren H, Coppens F, De Milde L, Muhlenbock P, Skiryecz A, Gonzalez N, Beemster GT, Inze D (2012) Exit from proliferation during leaf development in Arabidopsis thaliana: a not-so-gradual process. Dev Cell 22: 64-78

Pubmed: [Author and Title](#)

Google Scholar: [Author Only Title Only Author and Title](#)

Asl LK, Dhondt S, Boudolf V, Beemster GT, Beeckman T, Inze D, Govaerts W, De Veylder L (2011) Model-based analysis of Arabidopsis leaf epidermal cells reveals distinct division and expansion patterns for pavement and guard cells. Plant Physiol 156: 2172-2183

Pubmed: [Author and Title](#)

Google Scholar: [Author Only Title Only Author and Title](#)

Berckmans B, Lammens T, Van Den Daele H, Magyar Z, Bogre L, De Veylder L (2011) Light-dependent regulation of DEL1 is determined by the antagonistic action of E2Fb and E2Fc. Plant Physiol 157: 1440-1451

Pubmed: [Author and Title](#)

Google Scholar: [Author Only Title Only Author and Title](#)

Berckmans B, Vassileva V, Schmid SP, Maes S, Parizot B, Naramoto S, Magyar Z, Alvim Kamei CL, Koncz C, Bogre L, Persiau G, De Jaeger G, Friml J, Simon R, Beeckman T, De Veylder L (2011) Auxin-dependent cell cycle reactivation through transcriptional regulation of Arabidopsis E2Fa by lateral organ boundary proteins. Plant Cell 23: 3671-3683

Pubmed: [Author and Title](#)

Google Scholar: [Author Only Title Only Author and Title](#)

Bogre L, Magyar Z, Lopez-Juez E (2008) New clues to organ size control in plants. Genome Biol 9: 226

Pubmed: [Author and Title](#)

Google Scholar: [Author Only Title Only Author and Title](#)

Borghi L, Gutzat R, Futterer J, Laizet Y, Hennig L, Gruissem W (2010) Arabidopsis RETINOBLASTOMA-RELATED is required for stem cell maintenance, cell differentiation, and lateral organ production. Plant Cell 22: 1792-1811

Pubmed: [Author and Title](#)

Google Scholar: [Author Only Title Only Author and Title](#)

Borghi L, Gutzat R, Futterer J, Laizet Y, Hennig L, Gruissem W (2010) Arabidopsis RETINOBLASTOMA-RELATED Is Required for Stem Cell Maintenance, Cell Differentiation, and Lateral Organ Production. Plant Cell 22: 1792-1811

Pubmed: [Author and Title](#)

Google Scholar: [Author Only Title Only Author and Title](#)

Chen HZ, Tsai SY, Leone G (2009) Emerging roles of E2Fs in cancer: an exit from cell cycle control. Nat Rev Cancer 9: 785-797

Pubmed: [Author and Title](#)

Google Scholar: [Author Only Title Only Author and Title](#)

Clough SJ, Bent AF (1998) Floral dip: a simplified method for Agrobacterium-mediated transformation of Arabidopsis thaliana. Plant J 16: 735-743

Pubmed: [Author and Title](#)

Google Scholar: [Author Only Title Only Author and Title](#)

de Jager SM, Scofield S, Huntley RP, Robinson AS, den Boer BG, Murray JA (2009) Dissecting regulatory pathways of G1/S control in Arabidopsis: common and distinct targets of CYCD3;1, E2Fa and E2Fc. Plant Mol Biol 71: 345-365

Pubmed: [Author and Title](#)

Google Scholar: [Author Only Title Only Author and Title](#)

De Veylder L, Beeckman T, Beemster GT, de Almeida Engler J, Ormenese S, Maes S, Naudts M, Van Der Schueren E, Jacquard A, Engler G, Inze D (2002) Control of proliferation, endoreduplication and differentiation by the Arabidopsis E2Fa-DPa transcription factor. EMBO J 21: 1360-1368

Pubmed: [Author and Title](#)

Google Scholar: [Author Only Title Only Author and Title](#)

De Veylder L, Beeckman T, Inze D (2007) The ins and outs of the plant cell cycle. Nat Rev Mol Cell Biol 8: 655-665

Pubmed: [Author and Title](#)

Google Scholar: [Author Only Title Only Author and Title](#)

De Veylder L, Larkin JC, Schnittger A (2011) Molecular control and function of endoreplication in development and physiology. Trends Plant Sci 16: 624-634

Pubmed: [Author and Title](#)

Google Scholar: [Author Only Title Only Author and Title](#)

del Pozo JC, Diaz-Trivino S, Cisneros N, Gutierrez C (2006) The balance between cell division and endoreplication depends on E2FC-DPB, transcription factors regulated by the ubiquitin-SCF/SKP2A pathway in Arabidopsis. Plant Cell 18: 2224-2235

Pubmed: [Author and Title](#)

Downloaded from on November 22, 2019 - Published by www.plantphysiol.org
Copyright © 2019 American Society of Plant Biologists. All rights reserved.

Google Scholar: [Author Only](#) [Title Only](#) [Author and Title](#)

Dong J, MacAlister CA, Bergmann DC (2009) BASL controls asymmetric cell division in Arabidopsis. Cell 137: 1320-1330

Pubmed: [Author and Title](#)

Google Scholar: [Author Only](#) [Title Only](#) [Author and Title](#)

Doonan J, Hunt T (1996) Cell cycle. Why don't plants get cancer? Nature 380: 481-482

Pubmed: [Author and Title](#)

Google Scholar: [Author Only](#) [Title Only](#) [Author and Title](#)

Galinha C, Hofhuis H, Luijten M, Willemsen V, Bliou I, Heidstra R, Scheres B (2007) PLETHORA proteins as dose-dependent master regulators of Arabidopsis root development. Nature 449: 1053-1057

Pubmed: [Author and Title](#)

Google Scholar: [Author Only](#) [Title Only](#) [Author and Title](#)

Gazquez A, Beemster GTS (2017) What determines organ size differences between species? A meta-analysis of the cellular basis. New Phytol 215: 299-308

Pubmed: [Author and Title](#)

Google Scholar: [Author Only](#) [Title Only](#) [Author and Title](#)

Harashima H, Sugimoto K (2016) Integration of developmental and environmental signals into cell proliferation and differentiation through RETINOBLASTOMA-RELATED 1. Curr Opin Plant Biol 29: 95-103

Pubmed: [Author and Title](#)

Google Scholar: [Author Only](#) [Title Only](#) [Author and Title](#)

Henriques R, Magyar Z, Bogre L (2013) S6K1 and E2FB are in mutually antagonistic regulatory links controlling cell growth and proliferation in Arabidopsis. Plant Signal Behav 8: e24367

Pubmed: [Author and Title](#)

Google Scholar: [Author Only](#) [Title Only](#) [Author and Title](#)

Henriques R, Magyar Z, Monardes A, Khan S, Zalejski C, Orellana J, Szabados L, de la Torre C, Koncz C, Bogre L (2010) Arabidopsis S6 kinase mutants display chromosome instability and altered RBR1-E2F pathway activity. EMBO J 29: 2979-2993

Pubmed: [Author and Title](#)

Google Scholar: [Author Only](#) [Title Only](#) [Author and Title](#)

Heyman J, Van den Daele H, De Wit K, Boudolf V, Berckmans B, Verkest A, Alvim Kamei CL, De Jaeger G, Koncz C, De Veylder L (2011) Arabidopsis ULTRAVIOLET-B-INSENSITIVE4 maintains cell division activity by temporal inhibition of the anaphase-promoting complex/cyclosome. Plant Cell 23: 4394-4410

Pubmed: [Author and Title](#)

Google Scholar: [Author Only](#) [Title Only](#) [Author and Title](#)

Horiguchi G, Fujikura U, Ferjani A, Ishikawa N, Tsukaya H (2006) Large-scale histological analysis of leaf mutants using two simple leaf observation methods: identification of novel genetic pathways governing the size and shape of leaves. Plant J 48: 638-644

Pubmed: [Author and Title](#)

Google Scholar: [Author Only](#) [Title Only](#) [Author and Title](#)

Horvath BM, Kourova H, Nagy S, Nemeth E, Magyar Z, Papdi C, Ahmad Z, Sanchez-Perez GF, Perilli S, Bliou I, Pettko-Szandtner A, Darula Z, Meszaros T, Binarova P, Bogre L, Scheres B (2017) Arabidopsis RETINOBLASTOMA RELATED directly regulates DNA damage responses through functions beyond cell cycle control. EMBO J 36: 1261-1278

Pubmed: [Author and Title](#)

Google Scholar: [Author Only](#) [Title Only](#) [Author and Title](#)

Johnson DG, Schwarz JK, Cress WD, Nevins JR (1993) Expression of transcription factor E2F1 induces quiescent cells to enter S phase. Nature 365: 349-352

Pubmed: [Author and Title](#)

Google Scholar: [Author Only](#) [Title Only](#) [Author and Title](#)

Kalve S, De Vos D, Beemster GT (2014) Leaf development: a cellular perspective. Front Plant Sci 5: 362

Pubmed: [Author and Title](#)

Google Scholar: [Author Only](#) [Title Only](#) [Author and Title](#)

Karimi M, Inze D, Depicker A (2002) GATEWAY vectors for Agrobacterium-mediated plant transformation. Trends Plant Sci 7: 193-195

Pubmed: [Author and Title](#)

Google Scholar: [Author Only](#) [Title Only](#) [Author and Title](#)

Kobayashi K, Suzuki T, Iwata E, Magyar Z, Bogre L, Ito M (2015) MYB3Rs, plant homologs of Myb oncoproteins, control cell cycle-regulated transcription and form DREAM-like complexes. Transcription 6: 106-111

Pubmed: [Author and Title](#)

Google Scholar: [Author Only](#) [Title Only](#) [Author and Title](#)

Kobayashi K, Suzuki T, Iwata E, Nakamichi N, Chen P, Ohtani M, Ishida T, Hosoya H, Muller S, Leviczky T, Pettko-Szandtner A, Darula Z, Iwamoto A, Nomoto M, Tada Y, Higashiyama T, Demura T, Doonan JH, Hauser MT, Sugimoto K, Umeda M, Magyar Z, Bogre L, Ito M (2015) Transcriptional repression by MYB3R proteins regulates plant organ growth. EMBO J 34: 1992-2007

Pubmed: [Author and Title](#)

Google Scholar: [Author Only](#) [Title Only](#) [Author and Title](#)

- Kosugi S, Ohashi Y (2002) Interaction of the Arabidopsis E2F and DP proteins confers their concomitant nuclear translocation and transactivation. Plant Physiology 128: 833-843**
Pubmed: [Author and Title](#)
Google Scholar: [Author Only](#) [Title Only](#) [Author and Title](#)
- Li X, Cai W, Liu Y, Li H, Fu L, Liu Z, Xu L, Liu H, Xu T, Xiong Y (2017) Differential TOR activation and cell proliferation in Arabidopsis root and shoot apices. Proc Natl Acad Sci U S A 114: 2765-2770**
Pubmed: [Author and Title](#)
Google Scholar: [Author Only](#) [Title Only](#) [Author and Title](#)
- Magyar Z, Atanassova A, De Veylder L, Rombauts S, Inze D (2000) Characterization of two distinct DP-related genes from Arabidopsis thaliana. FEBS Lett 486: 79-87**
Pubmed: [Author and Title](#)
Google Scholar: [Author Only](#) [Title Only](#) [Author and Title](#)
- Magyar Z, Bogre L, Ito M (2016) DREAMs make plant cells to cycle or to become quiescent. Curr Opin Plant Biol 34: 100-106**
Pubmed: [Author and Title](#)
Google Scholar: [Author Only](#) [Title Only](#) [Author and Title](#)
- Magyar Z, De Veylder L, Atanassova A, Bako L, Inze D, Bogre L (2005) The role of the Arabidopsis E2FB transcription factor in regulating auxin-dependent cell division. Plant Cell 17: 2527-2541**
Pubmed: [Author and Title](#)
Google Scholar: [Author Only](#) [Title Only](#) [Author and Title](#)
- Magyar Z, Horvath B, Khan S, Mohammed B, Henriques R, De Veylder L, Bako L, Scheres B, Bogre L (2012) Arabidopsis E2FA stimulates proliferation and endocycle separately through RBR-bound and RBR-free complexes. EMBO J 31: 1480-1493**
Pubmed: [Author and Title](#)
Google Scholar: [Author Only](#) [Title Only](#) [Author and Title](#)
- Magyar Z, Meszaros T, Miskolczi P, Deak M, Feher A, Brown S, Kondorosi E, Athanasiadis A, Pongor S, Bilgin M, Bako L, Koncz C, Dudits D (1997) Cell cycle phase specificity of putative cyclin-dependent kinase variants in synchronized alfalfa cells. Plant Cell 9: 223-235**
Pubmed: [Author and Title](#)
Google Scholar: [Author Only](#) [Title Only](#) [Author and Title](#)
- Mariconti L, Pellegrini B, Cantoni R, Stevens R, Bergounioux C, Cella R, Albani D (2002) The E2F family of transcription factors from Arabidopsis thaliana. Novel and conserved components of the retinoblastoma/E2F pathway in plants. J Biol Chem 277: 9911-9919**
Pubmed: [Author and Title](#)
Google Scholar: [Author Only](#) [Title Only](#) [Author and Title](#)
- Matos JL, Lau OS, Hachez C, Cruz-Ramirez A, Scheres B, Bergmann DC (2014) Irreversible fate commitment in the Arabidopsis stomatal lineage requires a FAMA and RETINOBLASTOMA-RELATED module. Elife 3**
Pubmed: [Author and Title](#)
Google Scholar: [Author Only](#) [Title Only](#) [Author and Title](#)
- Morgan DO (2007) The Cell Cycle: Principles of Control. Oxford University Press**
Pubmed: [Author and Title](#)
Google Scholar: [Author Only](#) [Title Only](#) [Author and Title](#)
- Sadasivam S, DeCaprio JA (2013) The DREAM complex: master coordinator of cell cycle-dependent gene expression. Nat Rev Cancer 13: 585-595**
Pubmed: [Author and Title](#)
Google Scholar: [Author Only](#) [Title Only](#) [Author and Title](#)
- Saleh A, Alvarez-Venegas R, Avramova Z (2008) An efficient chromatin immunoprecipitation (ChIP) protocol for studying histone modifications in Arabidopsis plants. Nat Protoc 3: 1018-1025**
Pubmed: [Author and Title](#)
Google Scholar: [Author Only](#) [Title Only](#) [Author and Title](#)
- Simmons AR, Davies KA, Wang W, Liu Z, Bergmann DC (2019) SOL1 and SOL2 regulate fate transition and cell divisions in the Arabidopsis stomatal lineage. Development**
Pubmed: [Author and Title](#)
Google Scholar: [Author Only](#) [Title Only](#) [Author and Title](#)
- Sozzani R, Maggio C, Varotto S, Canova S, Bergounioux C, Albani D, Cella R (2006) Interplay between Arabidopsis activating factors E2Fb and E2Fa in cell cycle progression and development. Plant Physiology 140: 1355-1366**
Pubmed: [Author and Title](#)
Google Scholar: [Author Only](#) [Title Only](#) [Author and Title](#)
- Umbrasaitė J, Schweighofer A, Kazanaviciute V, Magyar Z, Ayatollahi Z, Unterwurzacher V, Choopayak C, Boniecka J, Murray JA, Bogre L, Meskiene I (2010) MAPK phosphatase AP2C3 induces ectopic proliferation of epidermal cells leading to stomata development in Arabidopsis. PLoS One 5: e15357**
Pubmed: [Author and Title](#)
Google Scholar: [Author Only](#) [Title Only](#) [Author and Title](#)

van den Heuvel S, Dyson NJ (2008) Conserved functions of the pRB and E2F families. Nat Rev Mol Cell Biol 9: 713-724

Pubmed: [Author and Title](#)

Google Scholar: [Author Only](#) [Title Only](#) [Author and Title](#)

White DW (2006) PEAPOD regulates lamina size and curvature in Arabidopsis. Proc Natl Acad Sci U S A 103: 13238-13243

Pubmed: [Author and Title](#)

Google Scholar: [Author Only](#) [Title Only](#) [Author and Title](#)

Xie Z, Lee E, Lucas JR, Morohashi K, Li D, Murray JA, Sack FD, Grotewold E (2010) Regulation of cell proliferation in the stomatal lineage by the Arabidopsis MYB FOUR LIPS via direct targeting of core cell cycle genes. Plant Cell 22: 2306-2321

Pubmed: [Author and Title](#)

Google Scholar: [Author Only](#) [Title Only](#) [Author and Title](#)

Yang K, Wang H, Xue S, Qu X, Zou J, Le J (2014) Requirement for A-type cyclin-dependent kinase and cyclins for the terminal division in the stomatal lineage of Arabidopsis. J Exp Bot 65: 2449-2461

Pubmed: [Author and Title](#)

Google Scholar: [Author Only](#) [Title Only](#) [Author and Title](#)

Zacksenhaus E, Jiang Z, Chung D, Marth JD, Phillips RA, Gallie BL (1996) pRb controls proliferation, differentiation, and death of skeletal muscle cells and other lineages during embryogenesis. Genes Dev 10: 3051-3064

Pubmed: [Author and Title](#)

Google Scholar: [Author Only](#) [Title Only](#) [Author and Title](#)

Zhang X, Henriques R, Lin SS, Niu QW, Chua NH (2006) Agrobacterium-mediated transformation of Arabidopsis thaliana using the floral dip method. Nat Protoc 1: 641-646

Pubmed: [Author and Title](#)

Google Scholar: [Author Only](#) [Title Only](#) [Author and Title](#)